Electrosorption of organic compounds: State of the art, challenges, performance, and perspectives

Navid Saeidi[1], Falk Harnisch[2], Volker Presser[3,4,5], Frank-Dieter Kopinke[1], Anett Georgi[1,*]

1. *Department of Environmental Engineering, Helmholtz Centre for Environmental Research – UFZ, 04318 Leipzig, Germany*
2. *Department of Environmental Microbiology, Helmholtz Centre for Environmental Research – UFZ , 04318 Leipzig, Germany*
3. *INM – Leibniz Institute for New Materials, 66123 Saarbrücken, Germany*
4. *Department of Materials Science and Engineering, Saarland University, 66123 Saarbrücken, Germany*
5. *saarene – Saarland Center for Energy Materials and Sustainability, 66123 Saarbrücken, Germany*

** Corresponding author contact information: Tel.: +49 341 235 1760; Fax: +49 341 235 1471; E-mail: anett.georgi@ufz.de*

Abstract

The widespread contamination of water resources with emerging organic contaminants necessitates the development of sustainable and cost-effective water treatment technologies. Adsorption, as a widely used water remediation process, is hampered by severe performance limitations against ionic and hydrophilic organic contaminants. In addition, no facile on-site regeneration techniques are available. Electrosorption of organic compounds (EOC) is a promising alternative to not only improve adsorption performance, but also to facilitate adsorbent regeneration by green electricity. The number of studies on EOC has grown exponentially over the past decades. There are numerous examples showing that applied electrical potentials can significantly enhance the adsorption affinity, capacity, and kinetics of conductive carbon adsorbents. However, whether these effects are specific to certain compound classes or more generally applicable remains unclear as well as the optimal criteria for designing EOC processes. Therefore, we critically evaluated the current state of the art of EOC in terms of active control of adsorption and desorption processes and the achievable effects for ionic and neutral organic compounds. Through a detailed consideration of compound speciation and surface chemistry of electrode materials, we derive mechanistic insights into the EOC process and discuss differences between electrosorption of inorganic and organic compounds. We provide definitions and propose insightful performance parameters to unify the rapidly growing EOC research. Potential application scenarios and future research directions are discussed. Overall, EOC is less likely to be a one-fits-all solution for removing contaminants, but adds a valuable tool especially for the hydrophilic and ionic organic contaminants that challenge conventional adsorption processes.

Keywords:

Organic pollutants; Electrosorption; Water treatment; On-site regeneration; Activated carbon; Nanomaterial.

Acronyms

2D	two-dimensional
AC	activated carbon
ACF	activated carbon felt
aD	amphoteric Donnan
BDD	boron-doped diamond
BT	complete breakthrough
CDI	capacitive deionization
CE	counter electrode
CNT	carbon nanotubes
CV	cyclic voltammetry
Cu/F-rGA	reduced graphene oxide aerogel loaded with Cu nanoparticles and fluorine
DeACF	defunctionalized ACF
EDL	electrical double-layer
EIS	electrochemical impedance spectroscopy
ELOX	electrooxidation
EOC	electrosorption of organic compound
GAC	granular activated carbon
GCS	Gouy-Chapman-Stern
HPPA	hydroxyphenyl propionic acid
HRT	hydraulic retention time or residence time
IHP	inner Helmholtz plane
IOC	ionic organic compound
mD	modified Donnan
MEC	microbial electrolysis cell
MET	microbial electrochemical technologies
MTBE	methyl tert-butyl ether
NOC	neutral organic compounds
OC	organic compound
OHP	outer Helmholtz plane
OXACF	oxidized ACF
PFAS	per- and polyfluorinated alkyl substances
PFBA	perfluorobutanoic acid
PFOA	perfluorooctanoic acid
PFOS	perfluorooctane sulfonic acid
pH_{PZC}	point of zero net proton charge
PMOC	persistent and mobile organic contaminant
PS1	pseudo-first-order
PS2	pseudo-second-order
p-TsO	p-tosylate
REACH	European Chemicals Regulation
RE	reference electrode
SDBS	dodecylbenzene sulfonate
SHE	standard hydrogen electrode
TFA	trifluoroacetic acid
TPA	tetrapropylammonium
WE	working electrode
WWTP	wastewater treatment plant

Symbols

$\Delta C_{A/B}$	change in capacitance per mol of adsorbed compound B
$\Delta H^{\varnothing}$	molar standard adsorption enthalpy
$\Delta G^{\varnothing}$	molar standard Gibbs energy of adsorption
$\Delta S^{\varnothing}$	molar standard adsorption entropy
ΔU_{el}	change in electrical energy
ε_0	permittivity of the vacuum
ε_r	dielectric constant
$\emptyset$	potential of electrode
$\emptyset_N$	potential drop induced by a permanent dipole moment
$\emptyset_N$	potential drop induced by a permanent dipole moment
C	specific capacitance
C_B	capacitance of the region/area occupied by 1 mol of an adsorbed organic compound
C_{des}	averaged contaminant concentration in the regeneration solution
C_e	concentration of solute dissolved in the aqueous phase at equilibrium
C_{in}	pollutant's inflow concentration
C_{out}	pollutant's effluent concentration

d	distance between the layer of counter ions and polarized surface
E	applied potential on WE
E_{eff}	effective potential
E_{OCP}	open circuit potential
E_{PZC}	potential of zero charge
F number	Faraday's number
K_0	sorption coefficient in the absence of applied potential
k_1	rate constant of PS1 model
k_2	rate constant of PS2 model
K (Ø)	potential-dependent sorption coefficient
K_C	dimensionless adsorption equilibrium constant
K_d	single-point sorption coefficient
$K_{d,\ BT}$	sorption coefficient at complete breakthrough
$K_{d,\ R}$	sorption coefficient calculated from retardation factor
K_F	Freundlich coefficient
$K_{F,\ des}$	Freundlich coefficient in desorption step
K_L	Langmuir adsorption coefficient
K_{SOC}	soil organic carbon–water distribution coefficients
m	mass
m_{ads}	amount of contaminant adsorbed
$m_{adsorbent}$	adsorbent (electrode) mass
m_{des}	total amount of adsorbate desorbed
m_{solid}	adsorbent mass
n	Freundlich exponent
n_{ads}	Freundlich exponent in adsorption step
n_{des}	Freundlich exponent in desorption step
Q	electric charge
q_{BT}	adsorption capacity at complete breakthrough
q_{charge}	charge accumulation
q_e	adsorbent loading at equilibrium
q_m	maximum (electro)sorption capacity
q_t	adsorbent loading at time t
R	universal gas constant
R factor	retardation factor
Re%	recovery percentage
S	integral area of the CV curve
S_B	surface area needed for one mol B to adsorb
T	absolute temperature
u_w	relative transport rate of water
v	scan rate
$V_{50\%\ ads}$	50%-breakthrough volume
$V_{95\%\ des}$	water volume needed in desorption to achieve 95% of the respective Re%
V_{ads}	breakthrough water volume
V_{BT}	complete breakthrough volume
V_{des}	volume of water for desorption
V_{in}	inflow volume
V_{void}	water-filled void volume of the adsorbent unit
X_{des}	degree of desorption or recovery

1. Introduction

Numerous sources of production, use, and disposal of chemicals commonly employed in medicine, industry, agriculture, and even common household conveniences, resulted in the widespread occurrence of emerging organic pollutants including very persistent micropollutants such as poly- and perfluorinated alkyl substances (PFAS) in the environment [1, 2].

Strategies to reduce this environmental burden include restrictions in use, point of source treatment, for example, for industrial or hospital effluents, and wastewater treatment plant (WWTP) optimization or tertiary treatment implementation [3, 4]. Among these approaches, activated carbon (AC) serving as a sorbent is currently an indispensable tool for reducing emissions of hardly biodegradable organic pollutants into the environment. The leading role of AC adsorption is based on its simplicity and safety in operation, long-lasting experience in water treatment applications, wide application range, and low cost of adsorbents. However, there are at least two critical aspects of using AC for the removal of the organic compounds:

I. There is an increasing concern about persistent and mobile organic contaminants (PMOCs) with freshwater half-lives longer than 40 days and soil organic carbon–water distribution coefficients of log K_{SOC} < 4.5 (at pH = 4–10) [5], which also challenge AC adsorption [6]. By 2019, nearly half of the organic compounds (OCs) registered under the European Chemicals Regulation (REACH) exhibit highly polar, ionic, or ionizable structures [5, 7]. Unlike conventional non-polar organic pollutants, PMOCs show low sorption to the soil, sediments, and technical adsorbents, including AC [6]. Incomplete removal by dosing powder ACs and an early breakthrough for fixed-bed carbon adsorbers have been reported for various PMOCs, including pharmaceuticals [8, 9] and short-chain perfluoroalkyl acids (PFAAs) [10, 11]. Higher amount of AC or more

frequent exchange of the AC bed in some cases may solve the problem, however at increased AC consumption.

II. Even though ACs are available at a relatively low cost, their use is associated with a significant environmental burden. Currently, on-site regeneration technologies for ACs are missing [12]. Thus, tons of granular AC (GAC) are transported over long distances (typically >> 100 km) to specialized high-temperature (> 800 °C) regeneration facilities or even incineration [12, 13]. Regarding CO_2 emissions, AC production alone is associated with a global warming potential of 8.6–18.3 kg eq CO_2 / kg AC during production. In addition, further emissions arise from transportation (e.g., 80% of AC consumed in Europe is imported) [14, 15]. Incineration and thermal regeneration are estimated to release 4.0 kg eq CO_2 / kg AC and 2.6 kg eq CO_2 / kg AC, respectively [16]. Thus, substantial positive economic and environmental impacts are anticipated for alternative technologies [12, 17].

Recent societal efforts toward a circular economy and energy transition from fossil to renewable energies also require new water treatment technologies. In this respect, electrochemical technologies can make an essential contribution as they can be operated in decentralized units with a small footprint and modular design. Electrochemical technologies can be easily automated, powered by renewables, and do not require chemicals' addition [18]. Tuning adsorption at conductive materials by applying external electric potentials (electrosorption) has received extensive interest, as it may allow combining minimization of waste and operational expenditures [19-21]. The first studies on electrosorption of inorganic ions on porous electrodes date back to the 1960s [22, 23], when it was used for desalting water, known these days as capacitive deionization (CDI). Thanks to the rapid and extensive growth evidenced by the many studies performed on CDI [24], scientific advances are

accompanied by increasing commercial development, where CDI technology is used by various global companies [21, 22, 24].

One of the first attempts for electrosorption of organic compounds (EOC) on porous electrodes was published in 1972 when Strohl and Dunlap studied the adsorption behavior of quinones on a polarized packed column of graphite particles as working electrode [25]. **Figure 1** illustrates the developments achieved in EOC from the 1970s to the present. It shows the number of published studies categorized by the charge state of the adsorbates under the experimental conditions applied.

While number of published papers on electrosorption of neutral organic compounds (NOCs) peaked around the millennium, the number of studies on the ionic organic compounds (IOCs) has enormously increased after 2010. The reason for this stronger interest could be the increasing demand for improved water treatment technologies for ionic substances as a significant subgroup of PMOCs.

In particular, EOC studies target three aspects that have been addressed as main challenges for efficient removal of OCs by adsorption from water [12, 26]: i) improving adsorption affinity and capacity, ii) enhancing adsorption kinetics, and iii) enabling *in situ* regeneration of the saturated adsorbents.

A recent review by Lissaneddine et al. [27] summarizes the available literature on EOC. It provides valuable insight into engineering aspects such as reactor design, up-scaling, and modeling. The present work aims to go beyond this in terms of the following aspects (as summarized in **Figure 1**), which we consider critical for evaluating the prospects of EOC for future water treatment:

- Adsorption capacity and affinity should be evaluated as performance indicators of electrosorption. Lissaneddine et al. [27] mainly focused on maximum electrosorption

capacities when listing the reviewed 37 studies in the field of EOC (**Table 1** in their review paper).

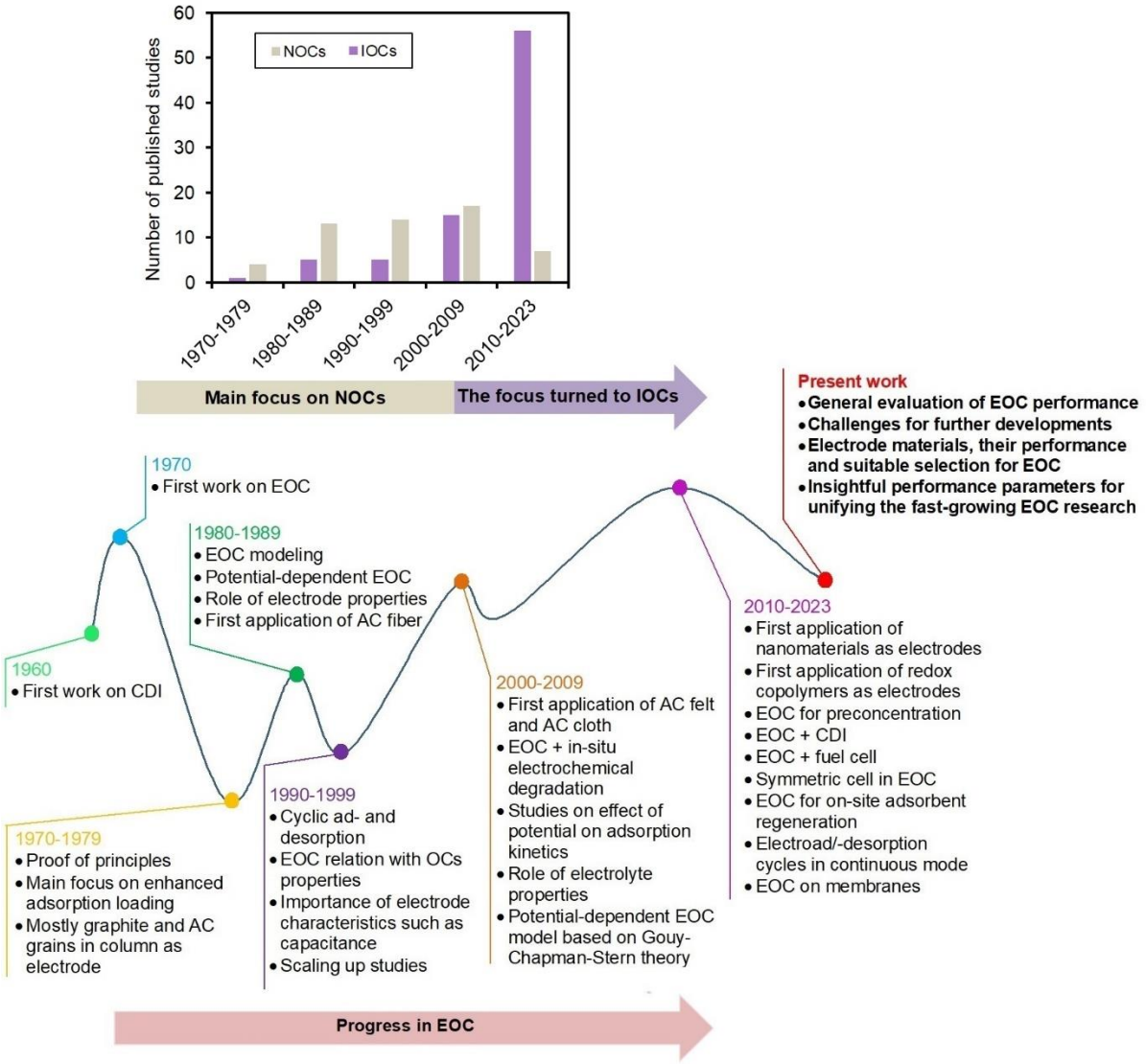

Figure 1. Timeline of scientific developments and working progress in EOC, followed by the aspects of the present work for further developments in EOC. Data on number of published papers focusing on neutral and ionic organic compounds (NOC and IOC) was obtained from Web of Science and Google Scholar.

Maximum adsorption capacity (q_m) is the equilibrium loading of the adsorbent with the target compound where no further uptake occurs due to the saturation of all available sorption sites. The *maximum capacity* is an important parameter for the adsorption of contaminants present in the mg/L range or above. However, when dealing with micropollutants present at trace level (µg/L range or below), adsorption *affinity* rather than *capacity* is the crucial performance parameter as q_m is usually not

reached by far. Sorption affinity is commonly described by the sorption coefficient K_d, that is, the concentration ratio of solute adsorbed on the adsorbent (q_e in mg/g) and dissolved in the aqueous phase (C_e in mg/L) at equilibrium. In the case of non-linear adsorption isotherms, K_d depends on the solute concentration, as detailed in **Section 3.2**. So far, despite the growing number of studies, a general evaluation of obtainable effects in the electrochemical enhancement of adsorption is still missing. In other words, by which magnitude can we change adsorption affinity and capacity and enhance adsorption kinetics of the adsorbent when applying a bias potential (a potential difference of typically 1.0-1.4 V called cell voltage or charging voltage).

- With the aim on using electrochemistry for on-site adsorbent regeneration, improvement of *ad*sorption is not the only (and maybe not even the most important) goal. Rather a strong modulation in the performance of ad- and desorption is desirable. Thus, changes in K_d and q_m under favorable and unfavorable charging conditions for solute adsorption need to be compared when applying different potentials. This also includes whether the effects of potentials at a specific material are related to specific compound classes, that is, only ionic or ionizable compounds, or apply to a broad compound range, including even neutrals.
- So far, the performance of electrodesorption for adsorbent regeneration has been evaluated by recovery percentage. The recovery percentage is calculated by comparing electrosorption capacities in reuse cycles: (amount of compound recovered by electrodesorption) / (amount of compound adsorbed) × 100 % [27, 28]. However, the recovery percentage in the flow-through fixed bed absorber is also related to the volume of water flushed through in the desorption step. Therefore, the enrichment factor is a more insightful parameter to assess electrodesorption performance, when

considering the ratio of water treated in the (electro)adsorption step and the concentrate volume received in the electrodesorption step.

- Adsorbent properties play a crucial role. For instance, the interactions of the adsorbate with intrinsic surface charges (i.e., due to pH-dependent protonation equilibria at open circuit potential (E_{OCP})), cannot be neglected when considering the effects of bias potentials [17, 28, 29].

Based on these aspects, our review evaluates the reported performance of EOC to address what we can expect from this technology in the future and what could be potential application scenarios of EOC in various water treatment tasks. Specific emphasis is placed on i) the impact of bias potential on adsorption affinity and capacity, ii) the role of target compound properties, iii) the effect of surface chemistry and textural properties of electrosorption electrodes on performance, and iv) essential parameters to be reported in electrosorption studies and suitable benchmarks for evaluation of EOC performance in both batch and continuous modes of operation. Thereby, we identify the challenges towards further improvements in EOC and propose future research and development directions.

2. Definitions and basic models: the solid/water interface

Electrosorption is based on the effects that an applied electric potential has on the sorption properties of a given material [30, 31]. Two effects are distinguished. For low potentials that is in the absence of redox reactions and only (pseudo)capacitive currents, the adsorption equilibrium of charged and uncharged molecules is shifted, as it is a function of the electric potential drop at the solid-liquid interface [32]. For high potentials, electrochemical redox reactions leading to Faradaic current occur in addition to equilibrium changes. This means that adsorbed molecules can be oxidized or reduced at the electrode, being possibly converted to more or less adsorbable products [33-36]. In some cases, full oxidation can also lead to carbon

dioxide and water formation. This can also be considered a post-treatment or decomposition step for *in situ* regeneration of an adsorbent saturated with OCs in a previous EOC step at low potentials [37, 38]. The present work focuses on the former effect as the main feature of EOC: the changes in reversible sorption equilibria when potentials are applied.

2.1. Electrical double-layer models and electrosorption of inorganic ions

At any interface between an electronic conductor (i.e., a solid or an immiscible liquid phase) and electrolyte solution, ion electrosorption occurs, and an electrical double-layer (EDL) is formed. At their interface, an excess electrical charge in the electrolyte solution being opposite to the excess charge in the solid conductor is present, and *vice versa*. At the same time, the whole interfacial system is charge neutral. When an external electric potential (that leads to an electrostatic field) is imposed on electrodes immersed in an aqueous electrolyte solution, ions in the electrolyte solution migrate into EDLs along the pore surfaces of the electrode/water interface. Ions are removed from the electrolyte solution bulk and are electrostatically held in the double layer until the discharging step, where the external power supply is shorted, or its polarity is reversed. The potential at which the electrode's charge is balanced without any local charge separation is the potential of zero charge (E_{PZC}).

Figure 2 illustrates essential models for describing ion uptake into the EDL, for example, a surface charged with cathodic potential. A physical EDL concept was formalized for the first time by Hermann von Helmholtz in the 19th century [39]. This model was later revised by Louis Gouy and David Chapman in 1910 and 1913, respectively [40, 41]. The Helmholtz model and the Gouy-Chapman model were combined into the widely utilized Gouy-Chapman-Stern (GCS) model by Otto Stern in 1924 (**Figure 2a**) [42]. The GCS model is based on the assumption of a planar, non-overlapping EDL typical for non-porous surfaces or sufficiently large pores. Here EDLs are formed at the interface of electron conductors and the electrolyte solution.

To obtain a large EOC adsorption capacity, materials with a high internal surface area of > 1000 m^2/g are typically used, such as nanoporous carbon materials [43]. When accounting for the electrochemically active surface area, micro-, meso-, and macropores of porous carbon electrodes are involved [44-46]. Macropores are dominantly responsible for the fast transport of ions. The electrolyte solution within macropores is assumed to be charge-neutral. Micropores (pore diameter d_p < 2 nm), due to their major contribution to the specific surface area, are considered as most important for electrosorption in porous carbon materials such as ACs [44-46].

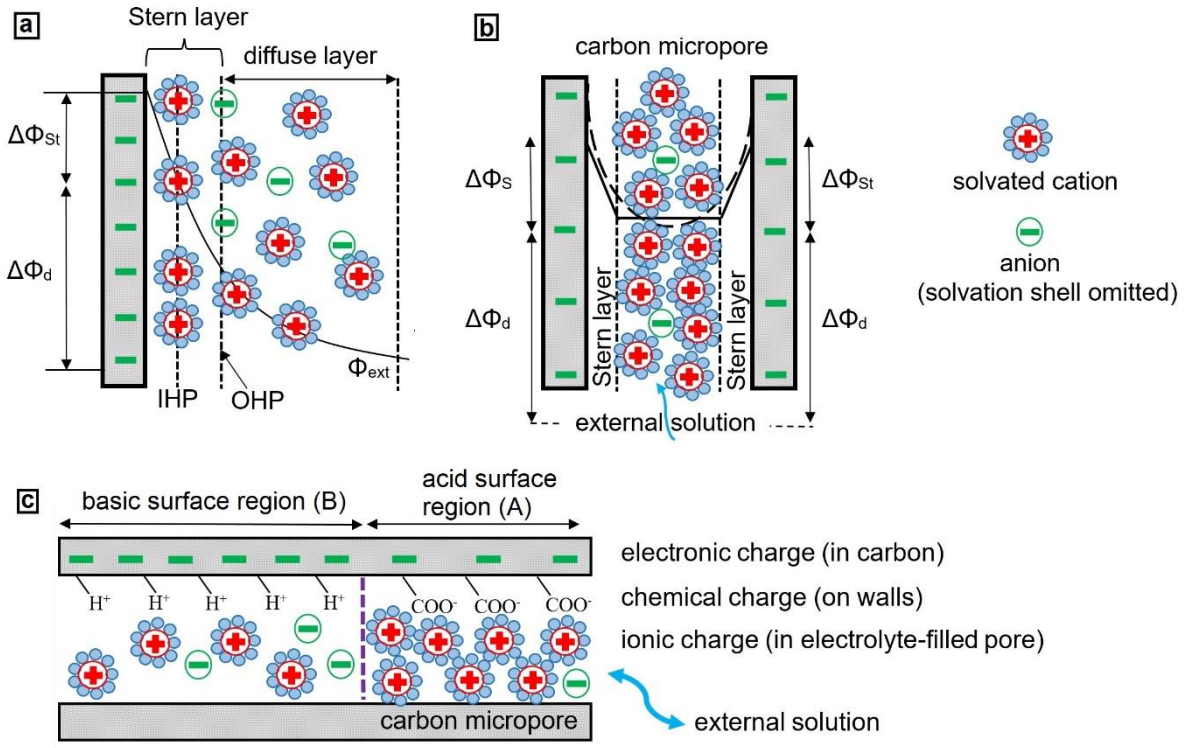

Figure 2. Various models for charge and potential distribution at charged surfaces and in micropores. (a) Stern model showing Inner Helmholtz plane (IHP) referring to the closest approach of specifically adsorbed ions and Outer Helmholtz plane (OHP) for the layer of non-specifically adsorbing ions. (b) Scheme of modified Donnan model (mD) for overlapping EDLs in micropores and (c) amphoteric Donnan model (aD) implementing the fixed chemical charge due to functional groups at an amphoteric surface (adapted from [45] and [44]).

Various models for describing charge compensation and ion storage in micropores have been proposed based on GCS and modified Donnan (mD) models [44, 45]. The latter considers ion storage to occur within the volume of micropores [47]. The mD model offers a simplified

approach, assuming full overlap of the diffuse layers in micropores with a uniform electric potential (**Figure 2b**) [45]. Mesopores have been shown to contribute to the ion electrosorption capacity of porous carbon electrodes with a significant portion of mesopores [46]. A two-dimensional porous electrode theory has been developed that is based on ion electrodiffusion through the interparticle pores in the electrodes and ion electrosorption in the intraparticle pores for materials with a fair amount of mesopores [46]. This model could be especially important for modeling EOC as molecule diameters of organic contaminants can span a wider range than inorganic ions and salts, emphasizing the importance of mesopores in EOC.

In addition to confinement, the presence of potentially charged functional groups depending on the local pH value in porous materials influences the EDL formation [48, 49]. Depending on precursor materials and production conditions, carbon materials such as ACs possess certain amounts of acidic (mainly carboxylic and phenolic) and basic surface groups. The latter result primarily from oxygen-free π-electron rich regions of the carbon backbone, which adsorb protons and/or certain N/O-functional groups [50, 51]. The amphoteric Donnan (aD) model, which is an advancement of the mD model, includes the impact of these fixed chemical charges and thus allows improved predictions on ion storage for carbon-based electrodes (**Figure 2c**). On the scale of nanometers or smaller size, regions influenced by basic surface sites ("B", left side of **Figure 2c**) are distinguished from regions influenced by carboxylic groups (acid, "A", right side of **Figure 2c**). The surface charge of the carbon can differ between the two regions and the ion composition in the aqueous phase [45]. Consequently, the applied electric potential of a sign opposite to the chemical surface charge first expels previously enriched counterions before reaching the E_{PZC}. Only after crossing the E_{PZC} the applied electric

charge leads to an effective accumulation of ions with the same sign as the chemical surface charge [48].

Consequently, the state of the net charge on a porous carbon electrode depends on both the applied external electric potential and the E_{PZC} of the electrode, that is, the 'surface chemistry'. **Figure 3** illustrates the state of the net charge on two carbon electrodes with different E_{PZC} as a function of applied potentials.

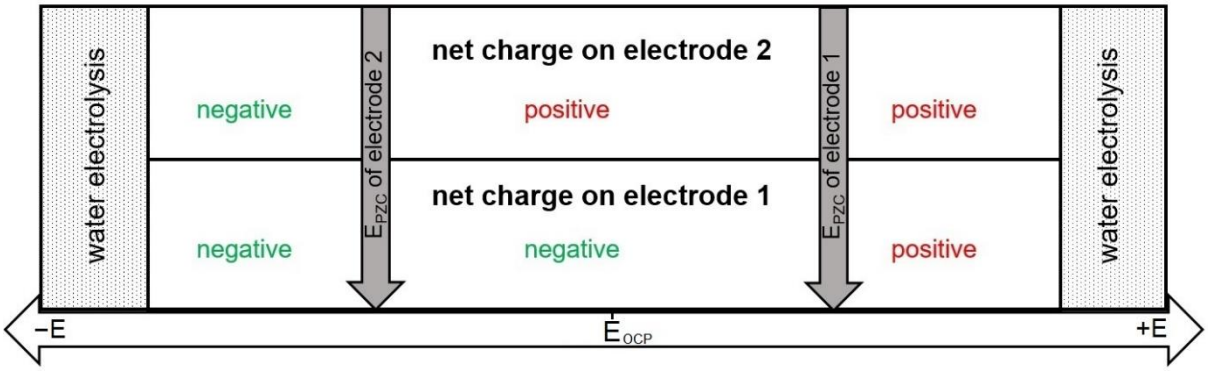

Figure 3. State of the net charge on two carbon electrodes with different E_{PZC} ($E_{PZC,\,1} > E_{PZC,\,2}$) vs. applied electric potential on WE (E) in an EOC cell. +E, –E, and E_{OCP} denote the anode potential, cathode potential, and open circuit potential, respectively. All potentials are vs. a reference electrode.

Even though this chemical charge is also called fixed charge in some studies [45, 49, 52], it is largely unclear whether and to which degree the applied electric potentials will affect the protonation/deprotonation equilibria of surface groups. One could hypothesize that protons adsorbed directly to the π-electron system (as the main source of positive 'fixed' charge on activated carbon materials) are more sensitive to an applied electric potential than chemically bound protons, which could only be influenced indirectly, for example, by mesomeric effects of carboxyl groups connected to aromatic rings. Protonation of carboxylic groups more distant from aromatic rings can be assumed even less prone to potential influence. However, more research is needed for a better mechanistic understanding of the complex interplay of electric and chemical charges on the electrode surface.

3. Definition and basic models: (electro)sorption of organic compounds

While significant progress was achieved in the last decade in the quantitative prediction of electrosorption of inorganic ions, model development for EOC is still in its infancy. One reason is the much higher complexity of involved interactions of OCs. The latter are generally larger molecules that can have specific features such as regions of localized charge combined with nonpolar regions (e.g., surface active compounds), pH-dependent charge due to dissociation equilibria of functional groups within the molecule (ampholytes), or even oppositely charged groups within one molecule (zwitterions). Thus, potential interactions with the solid surface are not just of electrostatic nature but can involve a variety of further non-specific (van-der-Waals) and specific interactions. The latter comprise, for example, π-π, n-π or ion-π interactions, H-bonding, and charge-assisted H-bonding or Lewis acid-base reactions [26].

Sorption coefficients (K_d, L/g or L/kg) describe the equilibrium between adsorbed and freely dissolved fractions of an adsorbate (**Eq. 1**), which is dependent on the change in free energy of the system during the adsorption process (**Eq. 2**).

$$K_d = \frac{q_e}{C_e} \quad (1)$$

where q_e (mg of adsorbate / g of adsorbent) is the adsorbent loading and C_e (mg/L) is the equilibrium concentration of the pollutant in the water phase at equilibrium.

$$RT \times \ln K_C = -\Delta G^{\varnothing} = -\Delta H^{\varnothing} + T \times \Delta S^{\varnothing} \quad (2)$$

In **Eq. 2**, K_C is the dimensionless adsorption equilibrium constant, R (8.314 J/(mol K)) the universal gas constant, T (K) the absolute temperature, $\Delta G^{\varnothing}$ (J/mol) the molar standard Gibbs energy of adsorption, $\Delta H^{\varnothing}$ (J/mol), and $\Delta S^{\varnothing}$ (J/(mol K) the standard adsorption enthalpy and entropy, respectively. We refer the readers to [53] for a discussion on how to convert K_d into the dimensionless K_C.

Driving forces for adsorption can arise from more favorable interactions (the enthalpy term) and a higher degree of freedom when the organic compound leaves the water phase and accumulates at the solid surface (the entropy term). The thermodynamically favorable interactions among water molecules are key drivers for the adsorption of hydrophobic compounds at surfaces, the so-called hydrophobic effect [26]. For instance, in PFAAs as organic anions, practically all adsorbents show increasing sorption with increasing carbon chain length, indicating that hydrophobicity contributes to their adsorption [54]. Different to inorganic ions, further non-electrostatic interactions of adsorbate and electrode surface can arise including van-der-Waals interactions, hydrogen bonding and π-π interactions [26].

Thus, compared to CDI, the complexity of the EOC process is an obstacle to developing predictive models. The doctoral thesis of Fischer [55] presented an approach to predict the impact of applied electric potential on sorption coefficients of OCs on AC based on the GSC model and the quantitative theory of Frumkin (1926) [56] which itself is based on the electrocapillary phenomenon. Frumkin's approach for the EDL considers the surface of the electron conductor and the layer of counterions (outer Helmholtz plane) to form a plate capacitor. Organic molecules being adsorbed to the surface and thus present in between the "plates of the capacitor" change its average dielectric constant, hence its internal electrical charge storage capacity. In this capacitor model, adsorption and desorption can be visualized by slabs of dielectric (water and pollutant) that move in and out between the plates. The change in electrical energy (ΔU_{el}) stored in the system when displacing water by organic adsorbates is calculated as:

$$\Delta U_{el} = -\frac{(\varepsilon_{r,A} - \varepsilon_{r,B}) \times \varepsilon_0 \times S_B \times \emptyset^2}{2 \times d} = -0.5 \times \Delta C_{A/B} \times \emptyset^2 \quad (3)$$

with indexes A used for water and B for the organic compound, respectively, ε_0 as the permittivity of the vacuum, ε_r as the dielectric constant of the compounds A and B, $\Delta C_{A/B}$ as

the change in capacitance per mol of adsorbed compound B in $\frac{C^2 \times S^2}{kg \times mol}$ or $\frac{F}{mol / m^2}$, and S_B is the surface area needed for one mole B to adsorb on, Ø as the potential of the electrode, and d as the distance between the layer of counter ions and polarized surface. Since values for ε_r can be derived from molecular properties, the derivation of **Eq. 3** is a significant result, as it theoretically predicts the effects of applied electric potential on the adsorptive behavior. As the dielectric constant of water is larger than that of organic molecules, the total electrical energy of the system is lower with water as dielectric material in the capacitor-like EDL. Thus, if the applied potential increases, the force pulling water inside (and pushing out the pollutant) increases. By applying this quantitative approach, Fischer [61] could explain the bell-shaped plots of sorption coefficients of OCs over the applied electric potential that were qualitatively predicted in an early study by Ban et al. [31] but rarely considered in later studies (**Figure 4**). Potential-dependent sorption coefficients K (Ø) can be derived from those determined experimentally in the absence of applied potentials (K_0) by **Eq. 4**:

$$K(Ø) = K_0 \times \exp\left\{\frac{-0.5 \times \Delta C_{A/B} \times Ø^2}{R \times T}\right\} \quad (4)$$

which is valid for OCs that do neither possess a permanent dipole moment nor adsorb in a specific orientation [55]. For such molecules, a term to account for an additional potential drop $Ø_N$ needs to be included, as shown in **Eq. 5**:

$$K(Ø) = K_0 \times \exp\left\{\frac{-0.5 \times \Delta C_{A/B} \times Ø^2 + C_B \times Ø_N \times Ø}{R \times T}\right\} \quad (5)$$

where C_B is the capacitance of the region/area occupied by 1 mol of an adsorbed organic compound. Fischer also predicted the shift in the maxima of K (Ø) vs. potential plots towards cathodic and anodic potentials for organic cations and anions, respectively. He applied a triple-layer model with contact-adsorbing ions as the third layer (that is the IHP). Contact-adsorbing

ions have specific ion-surface interactions beyond simple Coulomb attraction as typical for ionic organic compounds.

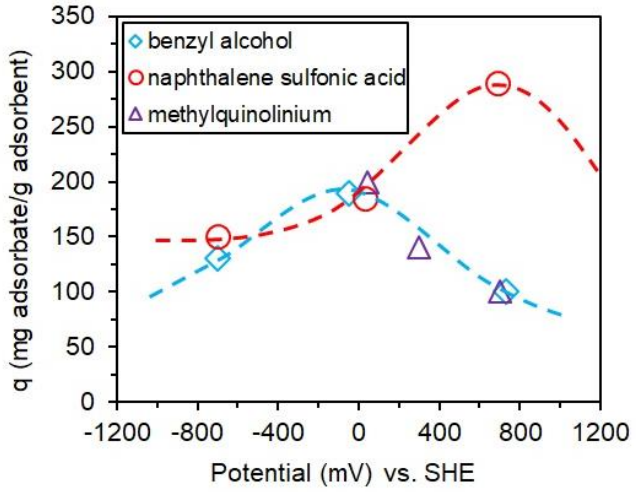

Figure 4. Electrosorption behavior of benzyl alcohol (in neutral form), naphthalene sulfonic acid (in anionic form) and methylquinolinium (in cationic form) on AC materials: symbols denote experimental data from [31], and lines denote the electrosorption behavior predicted by the model proposed by Fischer [55].

The capacity of a system where contact adsorption of ions takes place depends on the integral capacities of the inner and outer Helmholtz planes and the change in contact adsorption with electrode charge. Thus, the complex interactions of (larger) organic ions with the surface (as detailed above) certainly challenge quantitative predictions. When Fischer presented his work in 2001, scarce experimental data were available to verify model predictions [55]. This has changed, and bell-shaped curves of sorption performance indicators vs. potential were verified in various experimental studies, as explored in **Section 4.2.2**.

However, Fischer's model is based on the simple GCS model, which does not consider the role of pore size distribution of porous electrodes in EDL formation. Considering adsorbed molecules as a phase instead of individual molecules is another simplification of the model which might not hold for isolated adsorbate molecules or even thin adsorbate layers. Further to that Fischer considered the equations developed by Frumkin based on the Lippmann experiment [56], which investigated the electrosorption of organic compounds on a liquid mercury electrode. In the realm of electrochemical surface science, significant attention is

currently gained on unresolved issues that are critical for its future advancement, particularly regarding the electrocapillarity observed at solid-liquid interfaces [57]. Therefore, progress in modeling techniques can be attained by incorporating the latest advancements in electrocapillarity and EDL models (refer to **Section 2.1**).

4. Experimental practice and reported parameters in EOC studies

4.1. Determining the EOC potential window

The first experimental step for studying sorption equilibria in EOC is the selection of suitable potential windows, that is the minimum and maximum of the applied electrode potentials. First of all, any Faradaic process especially electrolysis of solvents should be avoided as it i) leads to parasitic energy consumption, ii) can hinder sorption processes by gas bubble formation inside the porous electrodes, iii) may lead to undesired chemical transformations of adsorbates due to the formation of reactive species, and iv) can cause electrode erosion. Therefore, the potential window is limited to values below water electrolysis. Thermodynamically, a potential bias of at least 1.23 V is required to electrolyze water under standard conditions [58].

In addition, the electrooxidation or electroreduction of OCs at the anode and cathode, respectively, are undesirable for reversible electroadsorption/electrodesorption. Cyclic voltammetry (CV) is often used to examine a suitable potential window and to study OCs' stability in a defined potential window [34, 35, 59, 60]. For redox-active compounds such as phenols or anilines with low standard oxidation potentials (typically 0.8 V to 1.1 V vs. SHE [61]), a suitable potential window without Faradaic currents can be limited to a relatively small range [34, 62]. On the contrary, some compounds, such as PFAAs, are stable in the whole potential window terminated only be water electrolysis on carbon electrodes, such as AC materials [29], carbon nanotubes (CNT) [63], and graphene [64]. However, the CV method is

not always applicable, and the results depend on the measurement parameters used. Especially small redox peaks for low concentrations of OCs in CV using high-capacity porous electrodes are hard to detect. In this case, determining the recovery of the original OC and/or screening for potential transformation products involving solvent extraction of the electrode/electrolyte after running chronoamperometry/-potentiometry for sufficiently long times seems an alternative.

4.2. EOC in batch mode experiments

EOC has been studied in batch mode frequently for providing proof of principle [29, 31, 55, 65], and elucidating electrosorption mechanisms [29, 31, 60, 66-74], as well as for studying performance of novel electrode materials [37, 63-65, 73, 75-80], potential-induced effects on adsorption equilibria [29, 31, 36, 70, 74, 81-83], and adsorption rates of OCs [70, 73, 78, 81-85]. Furthermore, some studies applied EOC in batch mode as a pre-step to derive essential parameters before performing a more technically relevant continuous mode [28, 31, 75, 86-89] or up-scaled electrosorption experiments [90].

A batch electrosorption cell includes a conductive porous electrode serving as an adsorbent (working electrode, WE) and a counter electrode (CE) [64, 65, 81]. A reference electrode (RE) is usually located close to the WE to control the potential applied on WE [17, 91]. A three-electrode system having different WE and CE is the most frequent case for running batch EOC [17, 29, 31, 64, 73, 92].

In general, efforts should be made to prevent interference from the CE in the electrosorption process, particularly in cases where the OCs involved may exhibit amphoteric properties. Additionally, it is crucial to ensure that during electrodesorption, the CE does not readsorb the target OCs that have been released from the working electrode. In case separating anode and

cathode, e.g. via membrane, is no option, using non-adsorbing CEs, for example, metal plates in undivided electrochemical cells or, reduces the complexity of the experimental system.

4.2.1. Effect of electric potential on adsorption equilibria: theoretical part

An advantage of batch experiments is that they allow equilibrium conditions so that the relevant parameters and conditions for evaluating EOC performance can be immedeatly calculated from the respective results. Conventionally, maximum (electro)sorption capacity (q_m) has been applied for assessing EOC performance. It can be calculated from (electro)sorption isotherms from batch experiments fitted with the Langmuir equation (**Eq. 6**) [93, 94] as one of the most frequently applied fitting models:

$$\frac{C_e}{q_e} = \frac{C_e}{q_m} + \frac{1}{q_m \times K_L} \quad (6)$$

where q_e (mg of adsorbate / g of adsorbent) is the electrode loading in equilibrium, q_m (mg/g) is maximum (electro)sorption capacity, C_e (mg/L) is the equilibrium concentration of the pollutant in the water phase, and K_L (L/g) is a constant related to the affinity between adsorbent and adsorbate. In general, for a good (electro)adsorption performance, a high q_m and a steep initial sorption isotherm, that is, a high (electro)sorption affinity (K_L here), are desirable.

In the case of micropollutants with trace concentrations in an aqueous solution, adsorption affinity is more decisive than maximum capacity, which might not be reached within the relevant range of C_e. If only the initial part of the isotherm is available, which can show significant curvature but still no clear plateau region, fitting by the Langmuir model is significantly error-prone. Instead, the empirical Freundlich equation (**Eq. 7**) [94, 95] is widely applied in such cases:

$$\log q_e = n \times \log C_e + \log K_F \quad (7)$$

where K_F ((mg/g)/(mg/L)^n) is the Freundlich constant related to the affinity between adsorbent and adsorbate, and n (dimensionless) is the Freundlich exponent.

Under certain conditions, it is useful to work with single-point sorption coefficients K_d (L/g or L/kg), which in the case of non-linear isotherms, are specific for a fixed point on the sorption isotherm defined by either C_e or q_e. It can be calculated from batch experiments or Freundlich and Langmuir isotherm parameters by **Eq. 8**:

$$K_d = \frac{q_e}{C_e} = C_e^{n-1} \times K_F = \frac{q_m}{1/K_L + C_e} \quad (8)$$

Single-point K_d values are useful for comparing the performance of different adsorbents for certain solute concentration conditions. This is not easily obvious from Freundlich or Langmuir fitting equations. **Eq. 8** was applied for obtaining the data presented in **Table 1**, in order to provide a comprehensive comparison of the published EOC data. To obtain clear information on adsorption affinity, K_d should be calculated at $q_e << q_m$ (e.g., $q_e \leq 0.3\ q_m$ was applied in [17]), that is, in the initial steep-slope part of electrosorption isotherms (q_e vs. C_e) so that the impact of limited capacity is rather low. The application of K_d values beyond the solute concentration range for which they were determined must be carefully considered.

4.2.2. Effect of potential on adsorption equilibrium: results and discussion

The basic assumption for applying EOC is that the bias potential modulates adsorption equilibria to higher or lower adsorption affinities and capacities, thus enhancing adsorption or desorption, respectively. This section summarizes experimental studies on potential-induced changes in adsorption equilibria in EOC. These studies were selected based on the following criteria: i) avoiding chemical transformations of analytes, that means no oxidation or reduction reactions thereof, ii) controlling and reporting pH values in the experiments and/or speciation of analytes at respective pH values, iii) no interference of CE in electrosorption, and iv) ensuring equilibrium conditions. Electrostatic attraction between cationic or anionic OCs

and oppositely charged porous electrodes has been frequently addressed as a mechanism for improved adsorption [28, 29, 31, 62, 63, 67, 71, 72, 77, 96-98]. Similarly, electrostatic repulsion by electrodes possessing a charge of the same sign as the ionic compounds was assigned to reduced adsorption [28, 29, 62, 70, 77, 97, 98]. Several studies also report significant effects of bias potential on the adsorption of OCs that are either non-ionizable or neutral under the defined experimental conditions (**Table 1**). In general, anodic bias potential can balance the negative chemical surface charge which is frequently occurring on ACs (caused by acidic surface groups [99]). This can result in stronger adsorption of NOCs [31, 55]. In the case of aromatic compounds, adsorption enhancement by anodic potentials was explained by stronger dispersion interactions between π-electrons of the aromatic ring and induced positive surface charges on ACs [82].

We assess the impact of electric potential on the adsorption equilibria of selected OCs (**Table 1** and **Figure 5**). Most authors reported and compared maximum adsorption capacities (q_m, calculated by fitting experimental data with the Langmuir equation (**Eq. 6**)). However, for micropollutant adsorption, the affinity below the maximum loading range is more important. Thus, we also calculated adsorption coefficients (K_d) from Freundlich isotherm parameters reported in the studies using **Eq. 8** at specific C_e values with $q_e << q_m$. In some of the studies in **Table 1**, no adsorption isotherm data were provided. In these cases, we report the adsorption loadings at equilibrium (q_e) from single-point adsorption experiments, as determined by the authors and calculated K_d using **Eq. 1**.

Table 1. Effect of bias potential on maximum adsorption capacities q_m (if available, otherwise q_e is reported [a]) and single-point adsorption coefficients K_d (in the low loading range, i.e. at $q_e < 0.3\ q_m$) for electrosorption of ionic and nonionic OCs on porous carbon electrodes based on literature data. Impact symbols assigned to the observed maximum potential effects in K_d: '+' < factor 2, '++' factor 2 to 10, '+++' > factor 10.

Compound	Compound speciation at considered pH [b] (in parentheses)	Adsorbent (WE)	q_m, (K_d) / adsorption or EOC at E_{OCP}	q_m, (K_d) / EOC at anodic potential [c]	q_m, (K_d) / EOC at cathodic potential [c]	Impact of potential on K_d	Reference
			q_m in mg/g and K_d in L/kg				
methyl tert-butyl ether (MTBE)	nonionizable	activated carbon felt (ACF)	-	9.22 [c], (K_d [d] 1,000) / +700 mV	9.90 [c], (K_d [d] 900) / +200 mV	+	[17]
nitrobenzene	nonionizable	ACF	454 [c], (K_d [d] 7400)	460 [c], (K_d [d] 8,000) / +650 mV	430 [c], (K_d [d] 5,150) / –160 mV	+	[85]
4-ethylphenol	Ionizable but neutral	AC fiber	-	0.0489, (K_d [e] 14.5) / +260 mV	0.174, (K_d [e] 43.0) / –450 mV	++	[100]
ethylbenzene	nonionizable	AC fiber	-	0.0478, (K_d [e] 16.0) / +260 mV	0.149, (K_d [e] 61.7) / –450 mV	++	[100]
hydroxyphenyl propionic acid (HPPA)	Ionizable but neutral	AC fiber	-	0.0665 (K_d [e] 16.8) / +260 mV	0.164, (K_d [e] 37.0) / –450 mV	++	[100]
benzyl alcohol	ionizable but neutral (7)	GAC	-	280, (K_d [e] 4,000) / +100 mV	265, (K_d [e] 2,200) / –600 mV	+	[55]
2-naphthol	ionizable but neutral (7)	ACF	-	500 [c], (K_d [d] 5,800) / +250 mV	390 [c], (K_d [d] 3,400) / –160 mV	+	[85]
p-chlorophenol	ionizable but neutral (7)	ACF	-	380 [c], (K_d [d] 3,300) / +250 mV	310 [c], (K_d [d] 2,400) / –160 mV	+	[85]
Phenol (1)	ionizable but neutral (7)	GAC	230, (K_d [e] 3,300)	260, (K_d [e] 6,500) / +700 mV	210, (K_d [e] 1,300) / –1000 mV	++	[55]
Phenol (2)	ionizable but neutral (6.5)	GAC	155, (K_d [e] 15,000)	200, (K_d [e] 25,000) / +1150 mV	140, (K_d [e] 6,000) / +50 mV	++	[86]
Phenol (3)	ionizable but neutral (5)	ACF	157, (K_d [e] 2,200)	259, (K_d [e] 6,400) / +1150 mV (cell voltage)	-	++	[92]
Phenol (4)	ionizable but neutral (7)	ACF	196 [c], (K_d [d] 1,400)	231 [c], (K_d [d] 2,300) / +650 mV	156 [c], (K_d [d] 1,100) / –160 mV	++	[85]
aniline	ionizable but neutral (6.5)	ACF	132, (K_d [e] 1,000)	401, (K_d [e] 3,500) / +850	-	++	[34]

m-cresol	ionizable but neutral (6.1)	ACF	246, (K_d [e] 1,300)	397, (K_d [e] 8,100) / +850 mV	-	++	[35]
resorcinol	ionizable but neutral (6.3)	ACF	65.4 [c], (K_d [d] 11,900)	69.4 [c], (K_d [d] 31,500)/ +800 mV	-	++	[82]
catechol	ionizable but neutral (6.1)	ACF	64.9 [c], (K_d [d] 11,800)	69.9 [c], (K_d [d] 79,400) / +800 mV	-	++	[82]
Phenol (5)	anionic (12.7)	ACF	18.4, (K_d [e] 170)	229, (K_d [e] 7,500) / +800 mV	-	+++	[59]
dodecylbenzene sulfonate (SDBS)	anionic (7)	ACF	-	620 [c], (K_d [d] 1,800) / +650 mV	460 [c], (K_d [d] 1,100) / –160 mV	+	[85]
naphthalenesul-fonic acid	anionic (7)	GAC	240, (K_d [e] 11,000)	330, (K_d [e] 20,000) / +800 mV	210, (K_d [e] 5,500) / – 400 mV	++	[31]
naphthoic acid	anionic (7)	GAC	175, (K_d [e] 10,000)	-	145, (K_d [e] 5,000) / – 400 mV	++	[31]
p-tosylate (1) (p-TsO)	anionic (7)	ACF	29.3, (K_d [e] 8,200)	35.1, (K_d [e] 15,300) / +700 mV	26.3, (K_d [e] 3,300) / +200mV	++	[17]
p-TsO (2)	anionic (7)	modified ACF	94.0, (K_d [e] 35,000)	98.8, (K_d [e] 60,000) / +600 mV	65.1, (K_d [e] 8,300) / –100 mV	+++	[17]
perfluorooctanoic acid (1) (PFOA)	anionic (6)	Cu / F-rGA	24.4, (K_d [e] 15,500)	37.1, (K_d [e] 140,000) / +1050 mV	-	+++	[101]
PFOA (2)	anionic (6.5)	CNT	290, (K_d [e] 140,000)	406, (K_d [e] 300,000) / +800 mV	-	++	[63]
PFOA (3)	anionic (6)	redox-copolymers	300 [c], (K_d [d] 11,500)	500 [c], (K_d [d] 53,000) / +1400 mV	120 [c], (K_d [d] 6,000) / –800 mV	+++	[65]
PFOA (4)	anionic (7)	ACF	21.5 [c], (K_d [d] 131,600)	24.1 [c], (K_d [d] 601,000) / +700 mV	15.20 [c], (K_d [d] 38,700) / –800 mV	+++	[29]
PFOA (5)	anionic (7)	modified ACF	35.7, (K_d [e] 200,000)	91, (K_d [e] 1,000,000) / +700 mV	11.7, (K_d [e] 40,000) / –800 mV	+++	[29]
PFOA (6)	anionic (3.6)	CNT/20% graphene	2.4, (K_d [e] 3,030)	492, (K_d [e] 54,000) / +800 mV	-	+++	[64]
PFBA (1)	anionic (7)	modified ACF	2.50, (K_d [e] 16,000)	2.57, (K_d [e] 18,000) / +450 mV	0.301, (K_d [e] 400) / –800 mV	+++	[29]
perfluorobutanoic acid (2) (PFBA)	anionic (7)	ACF	0.362, (K_d [e] 700)	0.374, (K_d [e] 850) / +700 mV	0.0647, (K_d [e] 50) / –800 mV	+++	[29]

perfluorooctane sulfonic acid (1) (PFOS)	anionic (6.5)	CNT	285, (K_d [e] 150,000)	470, (K_d [e] 450,000) / +800 mV	-	++	[63]
PFOS (2)	anionic (6)	redox-copolymers	225 [c], (K_d [d] 17,300)	500 [c], (K_d [d] 80,000) / +1400 mV	-	++	[65]
PFOS (3)	anionic (3.6)	CNT/20%graphene	6.3, (K_d [d] 11,400)	556, (K_d [d] 600,000) / +800 mV	-	+++	[64]
phenol red	anionic (7)	ACF	53.1, (K_d [e] 1,200)	57, (K_d [e] 1,450) / +650 mV	39, (K_d [e] 700) / –160 mV	++	[85]
acid orange 7	anionic (7)	ACF	378, (K_d [e] 2,700)	813, (K_d [e] 21,600) / +850 mV	-	+++	[36]
acid red 88	anionic (6)	graphene aerogel	154, (K_d [e] 72,000)	178, (K_d [e] 100,000) / +600 mV (cell voltage)	-	++	[73]
orange II	anionic (6)	graphene aerogel	153, (K_d [e] 83,000)	209 (K_d [e] 122,000) / +600 mV (cell voltage)	-	++	[73]
acid orange 8	anionic (6)	ACF	19.2 [c], (K_d [d] 6,000)	20.4 [c], (K_d [d] 28,000) / +1200 mV	-	++	[96]
acid yellow 14	anionic (6)	ACF	21.8 [c], (K_d [d] 6,100)	24.8 [c], (K_d [d] 37,000) / +1200 mV	-	++	[96]
acid red 151	anionic (6)	ACF	20.3 [c], (K_d [d] 44,500)	24.3 [c], (K_d [d] 54,00) / +1200 mV	-	++	[96]
2,4-D pesticide	98% anionic (5)	ACF	409 [c], (K_d [d] 11,600)	729 [c], (K_d [d] 24,100) / +1100 mV	291 [c], (K_d [d] 8,700) / –700 mV	++	[87]
sulfadimethoxine	90% anionic (6.8)	ACF	45.5 [c], (K_d [d] 450,000)	202 [c], (K_d [d] 21,000,000) / +1000 mV (cell voltage)	-	+++	[28]
bentazone	83% anionic (4)	ACF	18.1 [c], (K_d [d] 2,000)	26.1 [c], (K_d [d] 5,000) / +1200 mV	-	++	[66]
benzoic acid	55% anionic (4.3)	ACF	65 [c], (K_d [d] 5,700)	100 [c], (K_d [d] 23,000) / +800 mV	25 [c], (K_d [d] 1,300) / –700 mV	+++	[91]
tetrapropyl-ammonium (1) (TPA)	cationic (7)	ACF	47.5, (K_d [e] 11,400)	25.3, (K_d [e] 4,200) / +700 mV	79.2, (K_d [e] 57,000) / +200 mV	+++	[17]
TPA (2)	cationic (7)	modified ACF	33.9, (K_d [e] 13,000)	26.1, (K_d [e] 9,300) / +600 mV	128, (K_d [e] 100,000) / –100 mV	+++	[17]
tyrosine	cationic (0.7)	ACF	-	7.35, (K_d [e] 2,000) / +850 mV	8.86, (K_d [e] 6,400) / +50 mV	++	[100]

methylene blue (1)	cationic (6-7)	reduced graphene oxide/CNT	-	550 [c], (K_d [d] 10,000 L/kg) / –400 mV	731 [c], (K_d [d] 20,000) / –1000 mV	++	[76]
methylene blue (2)	cationic (6)	graphene aerogel	216, (K_d [e] 96,000)	219, (K_d [e] 150,000 L/kg) / –600 mV (cell voltage)	-	++	[73]
ciprofloxacin	cationic (6.8)	ACF	41.5 [c], (K_d [d] 350,000)		192 [c], (K_d [d] 200,000,000) / –1000 mV (cell voltage)	+++	[28]
clarithromycin	cationic (6.8)	ACF	13 [c], (K_d [d] 70,000 L/kg)		70.9 [c], (K_d [d] 74,000,000 L/kg) / –1000 mV (cell voltage)	+++	[28]
N-methyl-pyridinium	cationic (7)	ACF	1.98, (K_d [e] 900)	-	3.27, (K_d [e] 17,000) / –1000 mV	+++	[97]
ethylenediamine	87% cationic (10.5)	GAC	25.2, (K_d [e] 20)	22.9, (K_d [e] 60) / +500 mV	31, (K_d [e] 80) / –800 mV	++	[90]

[a] Reported capacity is from a single-point adsorption experiment conducted at a fixed initial concentration of adsorbate and quantity of adsorbent (WE) but applying different potentials. [b] Calculated using Chemaxon [102]. [c] All potentials are provided vs. SHE. [d] K_d was calculated from a single-point adsorption experiment conducted at a fixed initial concentration of adsorbate and quantity of adsorbent/electrode but at different potentials. [e] K_d was calculated for identical C_e values but different potentials using reported isotherms at adsorption capacity < 0.3 q_m. No index was given for maximum loadings determined from Langmuir isotherm data as directly obtained from the respective studies. Numbers in brackets after compound names are used to distinguish between different studies or experiments using the same compound.

These values may under- or overestimate the actual sorption affinities. In most cases, anionic compounds (24 studies) were investigated, followed by neutral (17) and cationic ones (9), as shown in **Table 1**. Especially in the case of anionic compounds, a larger number of studies dealt with improved adsorption only by applying anodic potentials (14) rather than with active control of ad- and desorption by studying anodic and cathodic potentials (10). Regarding neutral and cationic compounds, roughly half of the studies investigated more than one bias potential. The impact of bias potential on q_m is, in most cases, not larger than a factor of 2.5, possibly because q_m is limited by available surface area and pore volume.

Figure 5 shows the maximum observed enhancement factor in K_d when the bias potential was varied. The highest impact is generally found for ionic compounds.

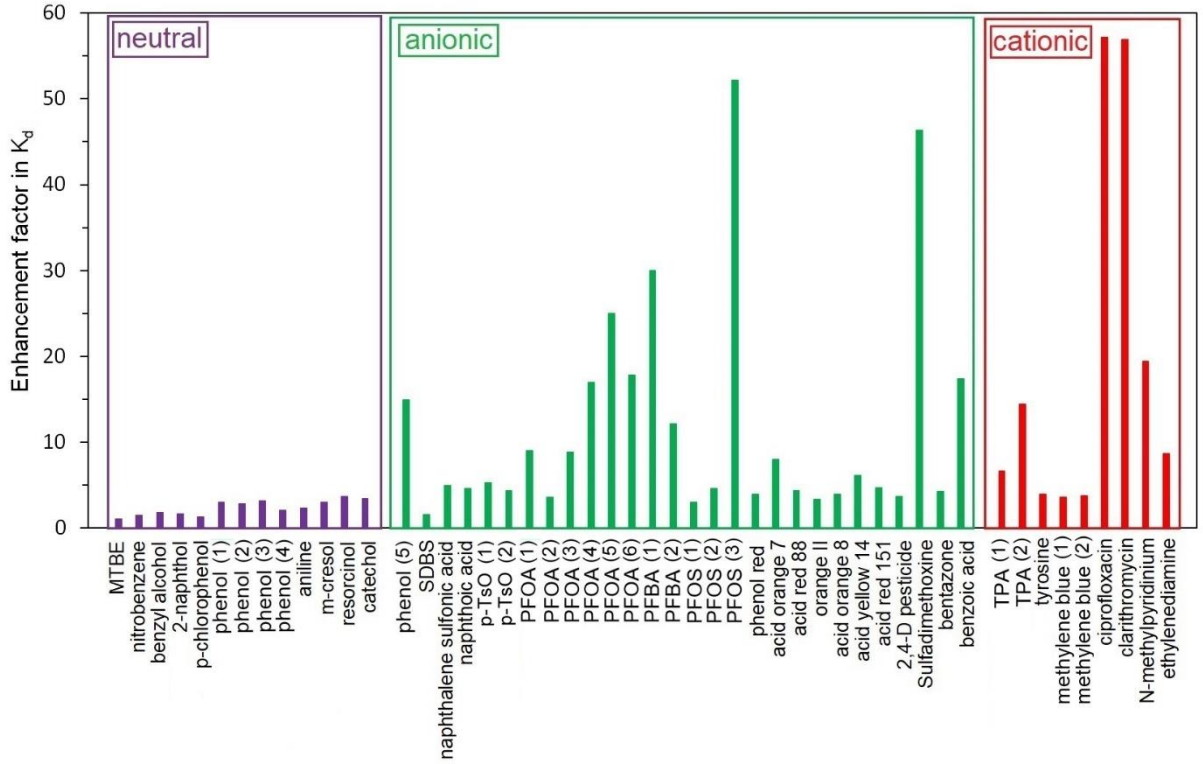

Figure 5. Maximum observed impact of bias potential on adsorption coefficients K_d of neutral, anionic, and cationic compounds. Numbers in brackets after compound names are used to distinguish between different studies or experiments using the same compound. For experimental conditions and references, see **Table 1**.

The variation in K_d with applied potential is generally below a factor of 3 for all neutral compounds listed in **Table 1**. This factor can rise to 50 or 60 for ionic compounds such as, for

example, for PFAAs [29] or cationic antibiotics [28]. Vastly different effects can be obtained in different studies for the same compound. Electrosorption of perfluorooctanoic acid (PFOA) on ACF and modified ACF (data sets addressed by PFOA (4) and PFOA (5), respectively) was influenced strongly as shown by variations in K_d up to a factor of 20 and 25, respectively, even in presence of 10 mg/L natural organic matter and increased ionic strength (up to 200 mM Na_2SO_4) [29]. A much lower impact of potential on PFOA adsorption was reported on CNT (factor 3.6, PFOA (2)) [63], reduced graphene oxide aerogel loaded with Cu nanoparticles and fluorine (Cu/F-rGA, PFOA (1)) (factor 9) [101], and redox copolymers (factor 8.8, PFOA (3)) [65]. Targeted surface chemistry modification of a commercial ACF increased potential-induced changes in K_d for PFBA (data set addressed by PFBA (1)) electrosorption up to a factor 30 [29]. Apparently, the exact experimental conditions have a substantial impact on EOC, most prominently the adsorbent (porous electrode) characteristics, applied potentials, and solution composition. In conclusion, there is only scattered knowledge. Thus, we advocate for standardization as detailed below to improve our understanding of impact of these parameters on EOC to allow leveraging finally its the technological potential.

Even though not considered in many studies, we could find 15 datasets from the EOC literature where a relatively wide potential range was studied with good resolution. **Figure 6** shows adsorption capacities (a) and adsorption coefficients (b) of some neutral, anionic, and cationic compounds (speciation at experimental conditions defined in the studies) vs. bias potentials on porous carbon electrodes. Bell-shaped curves were obtained by plotting the adsorption parameters vs. bias potential. Many curves have a distinct maximum and do not form a plateau as expected for saturation. This finding emphasizes that the simple assumption that, for example, cathodic potentials favor the adsorption of cationic OCs does not hold. Instead, there is an optimum potential for EOC, an essential parameter for any future application. This

optimum potential must be determined experimentally for the specific conditions in equilibrium batch experiments. Qualitatively, this behavior also agrees with the predictions of the model presented by Fischer [55] (**Section 3**). Thus, one should reconsider this work and critically evaluate its quantitative predictions based on a comparison with the increasing number of experimental EOC data in future model development.

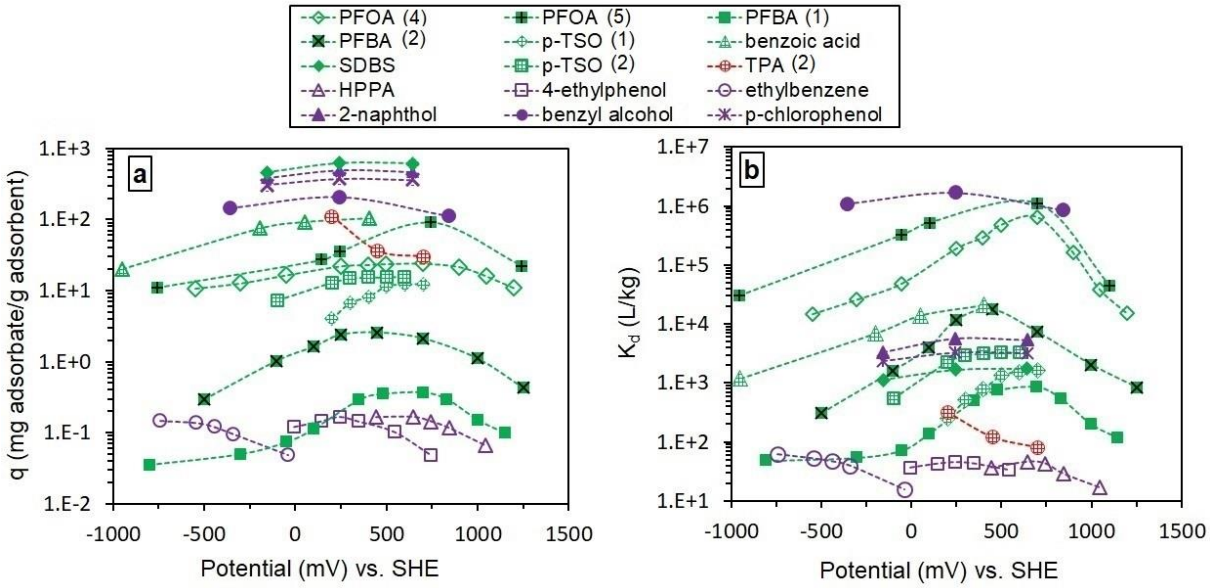

Figure 6. Adsorption capacities q (q_m or q_e) (a) and adsorption coefficients K_d (b) in EOC vs. applied potential on porous carbon electrodes from literature studies listed in **Table 1**. Purple symbols denote neutral, green symbols denote anionic, and red symbols denote cationic OCs. The curve of ethylbenzene adsorption shifted to the left by 300 mV, and the curve of HPPA adsorption shifted to the right by 300 mV for reason of better visibility. Lines serve as guides for the eye. Numbers in brackets after compound names are used to distinguish between different studies or experiments using the same compound. For experimental conditions and references, see **Table 1**.

As discussed in **Section 2.1.**, the state of the net charge on the carbon electrode is not necessarily identical with the sign of the bias potential. This is due to the superposition of electrically induced and permanent charges at the carbon surface (**Figure 2c**). The E_{PZC} is a characteristic of the electrode which depends on the surface chemistry of the electrodes and solution pH [29]. Most EOC studies did not consider E_{PZC} of the electrodes. For those with available E_{PZC} data, we converted **Figure 6** into **Figure 7**. In the latter, adsorption capacities (**Figure 7a**) and adsorption coefficients (**Figure 7b**) were plotted vs. the effective potential of the AC electrodes ($E_{eff} = E - E_{PZC}$) with E as the potential on WE. The highest adsorption

capacities and coefficients of anionic OCs are observed at $E_{eff} > E_{PZC}$, where the electrode net charge is positive. When E_{eff} is lower or higher than the peak potential, the adsorption performance decreases with a further decrease or increase in bias potential. For the potential region where both the surface and the adsorbate are negatively charged, electrostatic repulsion favors desorption. However, in the potential region with the opposite charge, the breakdown of adsorption is less easy to understand. This behavior is different from electrosorption of inorganic compounds and predicted by the capacitor model of the EDL being discussed in **Section 3**: Water molecules outcompete the adsorbates for adsorption on the highly positively charged surface sites [29, 55, 100]. Only one set of data for cationic OCs (adsorption of TPA on ACF) [17] shows the highest adsorption performance at E_{eff} moderately $< E_{PZC}$, while the adsorption parameters decrease significantly at $E_{eff} > E_{PZC}$.

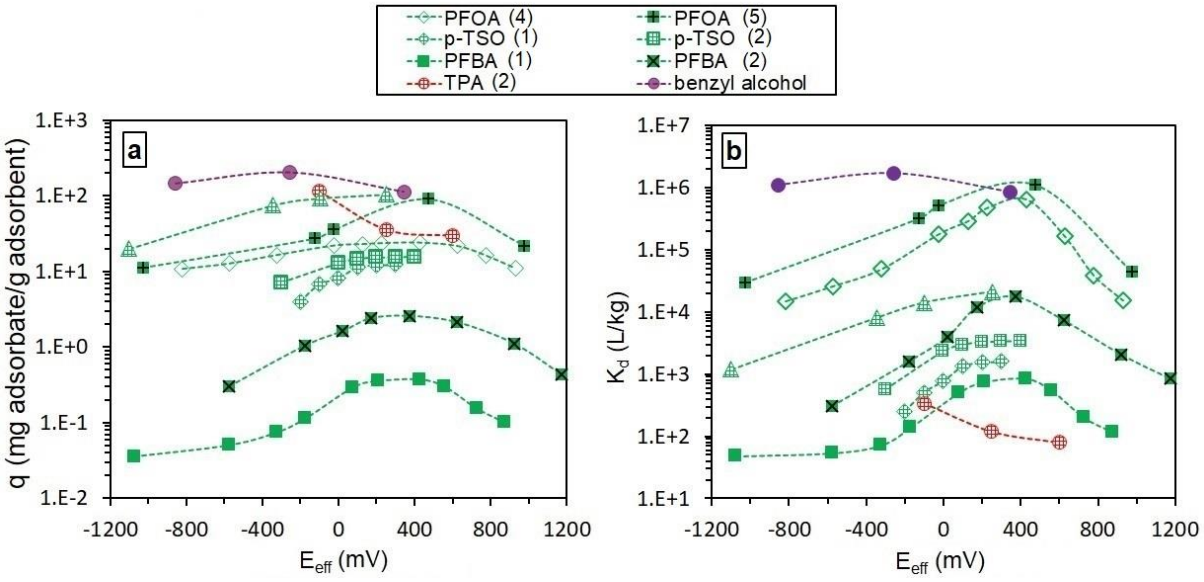

Figure 7. Adsorption capacities q (q_m or q_e) (a) and adsorption coefficients K_d (b) vs. E_{eff}. Purple symbols denote neutral, green symbols denote anionic and, red symbols denote cationic OCs. Lines serve as guides for the eye. Numbers in brackets after compound names are used to distinguish between different studies or experiments using the same compound. For experimental conditions and references, see **Table 1**.

The expected tendency for $E_{eff} < E_{PZC}$ cannot be proved by experimental data for cationic adsorbates, so far. Regarding benzyl alcohol as a neutral compound, the highest adsorption

performance is observed at E_{eff} close to E_{PZC}. An increase or decrease in potential lead to a drop in adsorption capacities.

In conclusion, we show that the E_{PZC} of the adsorbent is essential to understand EOC. Unlike electrosorption of inorganic compounds, specifying an effective potential is crucial for fully exploiting the potential of EOC. It also helps to run electroadsorption and -desorption at mild potentials, which protects carbon electrodes against oxidative attrition and preserves their performance for longer operation. The latter was discussed as a practical approach for prolonging the stable performance of CDI cells [48, 103].

AC materials, as the most widely applied electrodes for EOC, can also be selected or tailored for efficient EOC based on their E_{PZC} values. Various electrochemical methods have been applied in literature for determining E_{PZC} of electrodes in different electrolyte solutions, for example, measuring the immersion potential [104], chronoamperometry [105], cyclic voltammetry (at low scan rate) [106], and electrochemical impedance spectroscopy (EIS) at low frequency [107]. In our previous studies, E_{PZC} values of five ACFs (ACF1, ACF2, ACF3, and DeACF3 from [29], and OXACF2 from [17]) were determined using EIS under similar experimental conditions and at pH = 6-7. To create different surface chemistries, ACF2 was oxidized in 5 M nitric acid for 6 h at 90 °C to create additional carboxylate groups (OXACF2) [17]. In addition, ACF3 was reduced with H_2 at 900 °C to remove O-containing functional groups and create a basic surface (DeACF3) [29]. Textural properties of the ACFs were studied using nitrogen adsorption/desorption at –196 ˚C. All of the ACFs are predominantly microporous (micropore volume / total pore volume > 85%) with specific surface areas (BET) between 800 and 1500 m^2/g. The point of zero net proton charge (pH_{PZC}) of the ACFs was determined by the immersion method [99] and used to evaluate the state of chemical surface net charge on the ACFs at pH 7. **Figure 8a** shows surface area-normalized capacitance curves

vs. potential for all these ACF materials. The E_{PZC} values vary from +75 mV (vs. SHE) for DeACF3 to +620 mV for OXACF2. **Figure 8b** illustrates the effect of the chemical surface net charge of the ACFs on their E_{PZC} values. DeACF3 shows the highest pH_{PZC} = 9.3, and thus, the positive chemical net charge at pH 7 caused by protonation/deprotonation equilibria of its surface groups, has the lowest E_{PZC} of +75 mV.

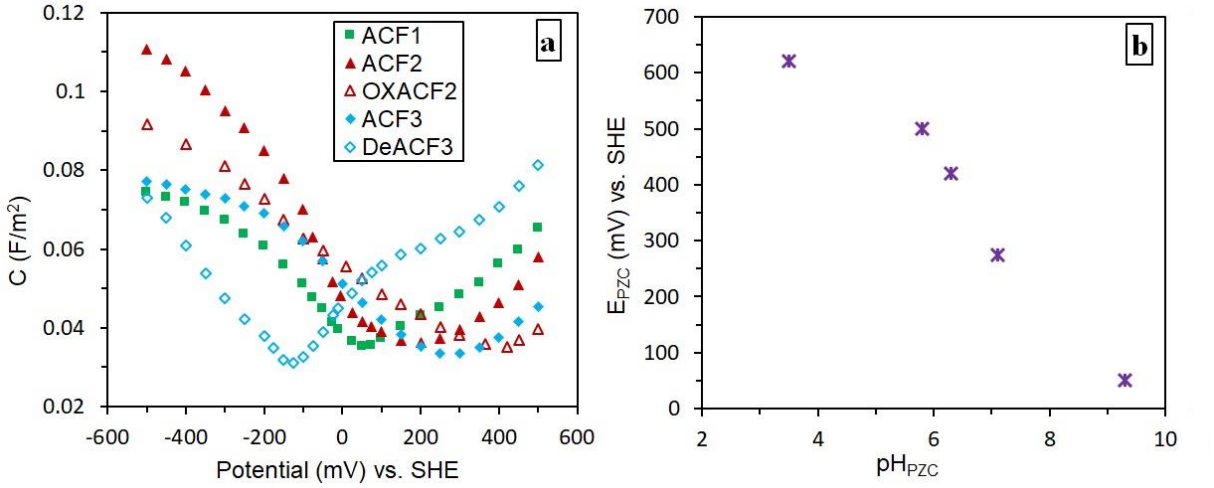

Figure 8. a) Surface area-normalized capacitance (C) of five ACFs at a frequency of 3.1 mHz vs. applied potential in 10 mM Na_2SO_4 at pH 6-7. The potential at minimum capacitance is considered E_{PZC}. b) Correlation of E_{PZC} and pH_{PZC}, illustrating the effect of ACF chemical surface net charge on E_{PZC}. ACF1, ACF2, ACF3, and DeACF3 from [29], OXACF2 from [17].

OXACF2 with pH_{PZC} = 3.5 and thus negative chemical net charge at pH 7, has the highest E_{PZC} of +620 mV, while a moderate E_{PZC} of +250 mV is observed for ACF1 with pH_{PZC} = 7.1, that is almost balanced chemical net charge at pH 7. This correlation between E_{PZC} and pH_{PZC} of AC materials has been addressed in CDI studies [48, 108] but, to the best of our knowledge, has not been considered in the field of EOC before. These results deliver two messages: i) E_{PZC} values of various electrode materials can differ widely, so it is necessary to know this parameter before using a specific material for EOC and ii) a simple determination of pH_{PZC} gives first information on the approximate location of E_{PZC} of the porous carbon electrodes. Knowledge of E_{PZC} and E_{OCP} of the porous electrodes can also be used to evaluate the net charge state. **Figure 9** shows the relation of the net charge state on the electrodes and the

E_{OCP} and E_{PZC} of the electrodes. With $E_{OCP} > E_{PZC}$ (electrode 1) the net charge on the electrode is positive. In contrast, for an electrode with $E_{OCP} < E_{PZC}$ (electrode 2), the net charge on the electrode is negative. This phenomenon helps to design ad/-desorption conditions by conducting one of the processes at E_{OCP}. For example, in the case of electrode 1, the adsorption of anionic OCs is improved at E_{OCP}. In contrast, electrode 2 favors the adsorption of cationic OCs at E_{OCP}.

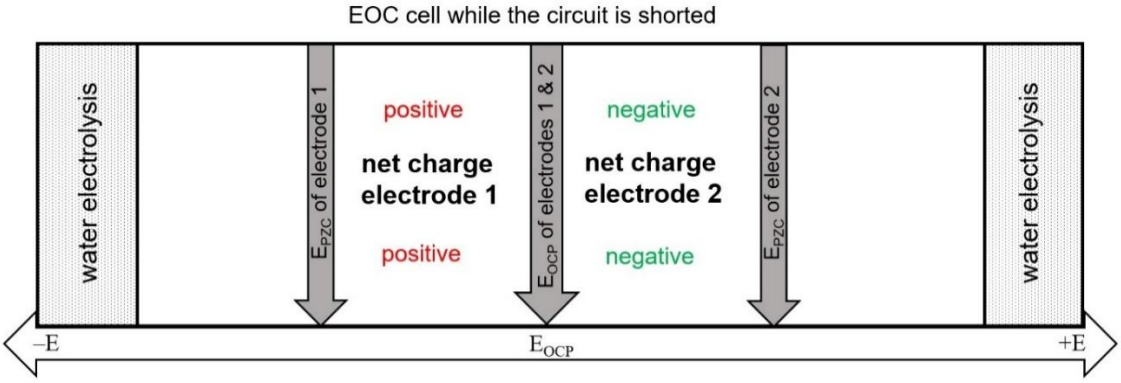

Figure 9. State of net charge on two porous electrodes at E_{OCP}. All potentials are vs. a reference electrode.

4.2.3. Effect of potential on adsorption kinetics

The effect of potential on the adsorption kinetics of OCs on porous electrodes can be evaluated from batch experiments. The pseudo-first-order (PS1, **Eq. 9**) [109] and pseudo-second-order (PS2, **Eq. 10**) [110] kinetics equations are most frequently applied. The respective rate constants k_1 and k_2 are, however, only empirical parameters obtained by fitting experimental data to the PS1 and PS2 models, respectively. The linearized form of PS1 is given as:

$$\ln (q_e - q_t) = -k_1 \times t + \ln (q_e) \quad (9)$$

where q_e and q_t (both in mg/g) are the amounts of adsorbate uptake per mass of adsorbent at equilibrium and at any time t (min), respectively, and k_1 (1/min) is the rate constant of the PS1 model with the start condition $q_{t=0} = 0$. By plotting $\ln (q_e - q_t)$ vs. t, the rate constant k_1 can be determined from the slope of the plot. The PS2 equation is given in its linearized form as:

$$\frac{t}{q_t} = \frac{t}{q_e} + \frac{1}{k_2 \times q_e^2} \quad (10)$$

where q_e, q_t, and t have the same meaning as in **Eq. 9**. k_2 in g/(mg × min) is the rate constant of the PS2 model. By plotting t/q_t vs. t, the rate constant k_2 can be calculated from the intercept.

The proposed rate laws are empirical [111] and the derived rate constants strongly depend on experimental conditions, including the agitation intensity and the degree of adsorption. In this respect, effective diffusion coefficients or surface diffusion coefficients for the transport of the adsorbate inside the porous solid would be more valuable as they are characteristic of a certain adsorbate/adsorbent pair [111, 112]. These are key parameters for intraparticle diffusion being a rate-determining step in most adsorption processes on porous adsorbents [111, 112] and thus should be used to interpret potential-induced effects on kinetics. However, such parameters can usually not be extracted from the reported kinetic data, and there is a strong prevalence of the PS1 and PS2 models in literature. To identify the effects of bias potential on adsorption kinetics, theier empirical rate constants k_1 and k_2 might still be applicable if otherwise identical experimental conditions in (electro)sorption experiments are maintained.

Table 2 shows the effect of potential on PS1 and PS2 adsorption rate constants of some anionic, cationic, and neutral compounds. All kinetic studies listed in **Table 2** applied bias potentials of opposite charges for anionic and cationic compounds. For neutral compounds, an anodic potential was applied (**Section 4.2.2.**).

The adsorption rates of neutral, anionic, and cationic compounds on porous carbon electrodes can, in some cases, be increased by applying a potential. As can be seen in **Figure 10**, anionic and cationic compounds are influenced more strongly than neutral compounds.

Table 2. Effect of bias potential on adsorption kinetics of various ionic and neutral OCs on porous carbon electrodes. Rate constants k_1 and k_2 are obtained from fitting to PS1 and PS2 models, respectively. Symbols assigned to observed factors in rate constants: 'n' no significant impact of potential, '+' < factor 2, '++' factor 2 to 10, '+++' > factor 10.

Compound	Compound speciation at considered pH [a] (in parentheses)	Adsorbent (WE)	k_x / adsorption or EOC at E_{OCP}	k_x / EOC	Impact of potential on adsorption rate constant	Reference
			k_1 in 10^{-3}/min and k_2 in g/(µmol h)			
nitrobenzene	nonionizable	ACF	k_1 = 15	k_1 = 38 / +644 mV	++	[85]
1,4-pyrazine	ionizable but neutral (7)	ACF	k_1 = 26.3	k_1 = 27.3 / +5 mA (galvanostatic mode)	n	[97]
1-quinoline	ionizable but neutral (7)	ACF	k_1 = 51.2	k_1 = 57.8 / +5 mA (galvanostatic mode)	+	[97]
2,2-bipyridyl	ionizable but neutral (7)	ACF	k_1 = 78.8	k_1 = 83.1 / +1 mA (galvanostatic mode)	n	[68]
4,4-bipyridyl	ionizable but neutral (7)	ACF	k_1 = 58.9	k_1 = 63.2 / +1 mA (galvanostatic mode)	n	[68]
phenol	ionizable but neutral (7)	ACF	k_1 = 81	k_1 = 63 / +850 mV	+	[85]
aniline	ionizable but neutral (6.5)	ACF	k_1 = 5.35	k_1 = 7.11 / +800 mV	+	[34]
m-cresol	ionizable but neutral (6.1)	ACF	k_1 = 6.38	k_1 = 11.3 / +850 mV	+	[35]
resorcinol	ionizable but neutral (6.3)	ACF	k_1 = 2.28	k_1 = 6.97 / +800 mV	++	[82]
catechol	ionizable but neutral (6.1)	ACF	k_1 = 5.60	k_1 = 9.4 / +600 mV	+	[82]
phenol	anionic (12.7)	ACF	k_1 = 4.81	k_1 = 8.20 / +950 mV	+	[59]
PFOA (1)	anionic (6)	Cu / F-rGA	k_1 = 0.0610	k_2 = 0.157 / +1000 mV	++	[101]
PFOA (2)	anionic (6.5)	CNT	k_2 = 680	k_2 = 810 / +800 mV	+	[63]
PFOA (3)	anionic (3.6)	CNT/20%graphene	k_2 = 0.0367	k_2 = 0.356 / +800 mV	++	[64]
PFOA (4)	anionic (7)	ACF	k_2 = 73.3	k_2 = 72.9 / +700 mV	n	[29]
PFOS (1)	anionic (6.5)	CNT	k_2 = 520	k_2 = 1,290 / +800 mV	++	[63]
PFOS (2)	anionic (3.6)	CNT/20%graphene	k_2 = 0.0468	k_2 = 0.595 / +800 mV	+++	[64]
phenol red	anionic (7)	ACF	k_1 = 0.5	k_1 = 2 / +600 mV	++	[85]
Dodecylbenze-ne sulfonate (SDBS)	anionic (7)	ACF	k_1 = 16	k_1 = 19 / +650 mV	+	[85]
acid orange 7	anionic (7)	ACF	k_1 = 4.47	k_1 = 9.81 / +850 mV	+	[36]
acid red 88	anionic (6)	graphene aerogel	k_2 = 80	k_2 = 210 / +600 (cell voltage)	++	[73]
orange II	anionic (6)	graphene aerogel	k_2 = 180	k_2 = 560 / +600 (cell voltage)	++	[73]
acid orange 8	anionic (6)	ACF	k_1 = 28.1	k_1 = 34.8 / +1250 mV	+	[96]
acid yellow 14	anionic (6)	ACF	k_1 = 26	k_1 = 23 / +1250 mV	n	[96]

acid red 151	anionic (6)	ACF	k_1 = 16.2	k_1 = 19.0 / +1250 mV	+	[96]
bentazone	83% anionic (4)	ACF	k_1 = 1.5	k_1 = 6.5 / +1000 mV	++	[66]
benzoic acid (1)	54% anionic (3.6)	ACF	k_1 = 35.1	k_1 = 43.4 / +800 mV	+	[62]
benzoic acid (2)	55% anionic (4.3)	ACF	k_1 = 35.5	k_1 = 42.3 / +1100 mV	+	[91]
phthalic acid	92% anionic (4)	ACF	k_1 = 34.0	k_1 = 46.9 / +1100 mV	+	[91]
nicotinic acid	91% in zwitterionic and 7% in anionic form (4.5)	ACF	k_1 = 28.8	k_1 = 51.5 / +1100 mV	+	[91]
crystal violet	cationic (3.6)	ACF	k_1 = 2.4	k_1 = 12.5 / –1050 mV	++	[70]
basic blue 7 (1)	cationic (3.6)	ACF	k_1 = 3.9	k_1 = 12.5 / –600 mV	++	[70]
basic blue 7 (2)	cationic (6.3)	ACF	k_1 = 2.4	k_1 = 9.0 / –2 mA (galvanostatic mode)	++	[72]
basic blue 11	cationic (3.6)	ACF	k_1 = 8.51	k_1 = 13.9 / –600 mV	++	[70]
methylene blue	cationic (6)	graphene aerogel	k_2 = 3,600	k_2 = 3,630 / –600 mV (cell voltage)	n	[73]
2,2-bipyridyl (1)	cationic (1.7)	ACF	k_1 = 60.8	k_1 = 69.4 / –1 mA (galvanostatic mode)	+	[68]
2,2-bipyridyl (2)	cationic (1.7)	ACF	k_1 = 30.8	k_1 = 44.8 / –1 mA (galvanostatic mode)	+	[68]
N-methyl-pyridinium	cationic (7)	ACF	k_1 = 10	k_1 = 47 / –1 mA (galvanostatic mode)	++	[97]
pyridinium	cationic (7)	ACF	k_1 = 7.41	k_1 = 24.5 / –1 mA (galvanostatic mode)	++	[97]

[a] Calculated using Chemaxon [102]. EOC experiments were performed in potentiostatic mode, when not mentioned otherwise. Numbers in brackets after compound names are used to distinguish between different studies or experiments using the same compound. All potentials are provided vs. SHE.

This was also illustrated by a study using two nitrogen heterocyclic aromatic compounds (4-pyrazine and 1-quinoline) in their neutral and cationic forms [97]: ACF cathodic potential has a greater effect on cationic than neutral molecule adsorption rates. When mainly microporous ACs were applied as absorbents (e.g., PFOA (4)), the effect of potential on the adsorption rates was moderate or even insignificant

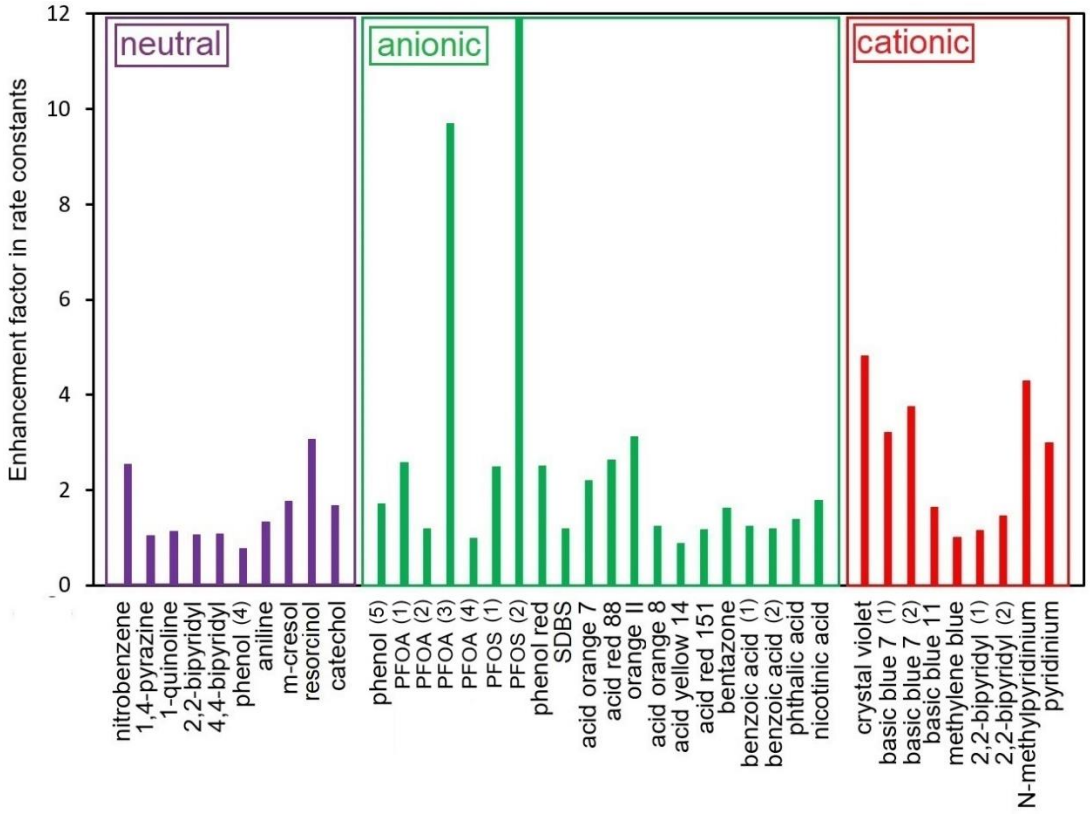

Figure 10. Impact of potential on adsorption rate of neutral, anionic, and cationic compounds on porous carbon electrodes evaluated by the observed enhancement factors in adsorption rate constants (k_1 or k_2) with and without applied bias potential. For experimental conditions and citations, see **Table 2**. Bias potential of opposite charges was applied for anionic and cationic compounds, while an anodic potential was applied in all cited studies on neutral compounds. Numbers in brackets after compound names are used to distinguish between different studies or experiments using the same compound.

At the same time, the strongest enhancing effects were reported for PFOA (2) and PFOS (1) electrosorption on CNT/20%graphene composite (mean pore diameter of CNT as the main component (80%) of the composite: 3.1 nm). Micropores (< 2 nm) and especially sub-nanometer pores smaller than 0.8 nm can pose severe limitations on ion transport in CDI flow cells [46, 113]. In CDI, the choice for the best electrode pore size depends on the ion size and

interplay of solvation [113, 114]. In terms of accessibility of micropores for OCs, the situation is more complex than for inorganic ions due to their wider structural variability. While kinetic diameters of organic molecules are sometimes used, this parameter is not reflecting the actual molecular dimensions [115]. The dimension of the adsorbate that is critical for entry into a pore depends on the shape of the pore as well as the geometry of the molecule. For example, in slit-shaped pores the molecule size in the minimum dimension, will determine, if it can enter the pore. In cylindrical pores, the size of the molecule in two dimensions must be considered. In this respect, effective diameters are used which can be understood as the minimum diameter of a cylinder circumscribing the molecule. However, such data are not widely available in tabulated form for OCs, yet. Effective diameters of OCs reach from about 0.45 nm for simple *n*-alkanes to several nm e.g. for dye molecules or antibiotics [116]. In CDI, porous electrodes that combine a large micropore volume (for a high deionization capacity) with a network of mesopores (between 2 nm and 50 nm) and macropores (> 50 nm) were recommended for highly efficient deionization. The electrode design should encompass intraparticle pore design and particle packing/arrangement to control the interparticle pore volume [114, 117, 118]. Further discussions on the effect of porosity on the adsorption kinetics of OCs when applying a potential can be found in **Section 6**. However, a comprehensive investigation of the effect of the pore size distribution of the porous electrodes on EOC is an interesting future research subject.

Polarization effects on the adsorption rate of OCs can arise from changes in surface charge density and the associated changes in the orientation of water dipoles and the strength of their electrostatic attraction, which can more or less hinder pore diffusion of the adsorbate [63, 68, 97]. Also, stronger adsorption of the adsorbate to the charged surface can slow down its diffusion inside the porous solid. In the future, mechanistic discussions on the effect of the

electric potential on adsorption kinetics should be based on surface or effective intraparticle diffusion rate coefficients instead of empirical rate constants as explained above. So far, only the study by Sun et al. [73] considered intraparticle diffusion rate constants (calculated by the Weber and Morris model [119]) of three anionic dye compounds on three-dimensional graphene aerogel and reported a moderate increase of factor 1.4 upon anodic polarization. Kinetics of potential-driven desorption steps were not considered in the great majority of the literature studies calling for more detailed research thereon. Furthemore, the role of adsorbate molecular structure on EOC was rarely considered. Bayram and Ayranci [62] found that the decrease in extent of potential effect on adsorption rates of nicotinic acid, phthalic acid, and benzoic acid is in order of their dipole moments (3.05 D > 2.59 D > 1.21 D, respectively). **Figure 10** illustrates a wide variability in the effects observed for different compounds of the same charge, which can, however, be superimposed by differences in the applied adsorbents. Thus, future studies using for example a wide range of compounds with the same adsorbent material are needed in order to derive solid mechanistic conlcusions on the role of molecular structure in EOC.

5. EOC in continuous mode

In addition to operating charge/discharge cycles in batch mode, EOC has also been explored for continuous operation [25, 28, 62, 80, 86-91, 98, 100, 120-123]. Flow-through and flow-by plate electrode cells or packed beds have been applied. For detailed information on flow cell types and configurations, we refer the reader to Lissaneddine et al. [27]. Here, we aim to add an evaluation of EOC performance in flow mode and discuss which parameters are insightful indicators for the performance of continuous EOC in enhanced electro-assisted adsorption and desorption (electrode regeneration), including the enrichment of targeted OCs in the regeneration concentrate (**Figure 11**).

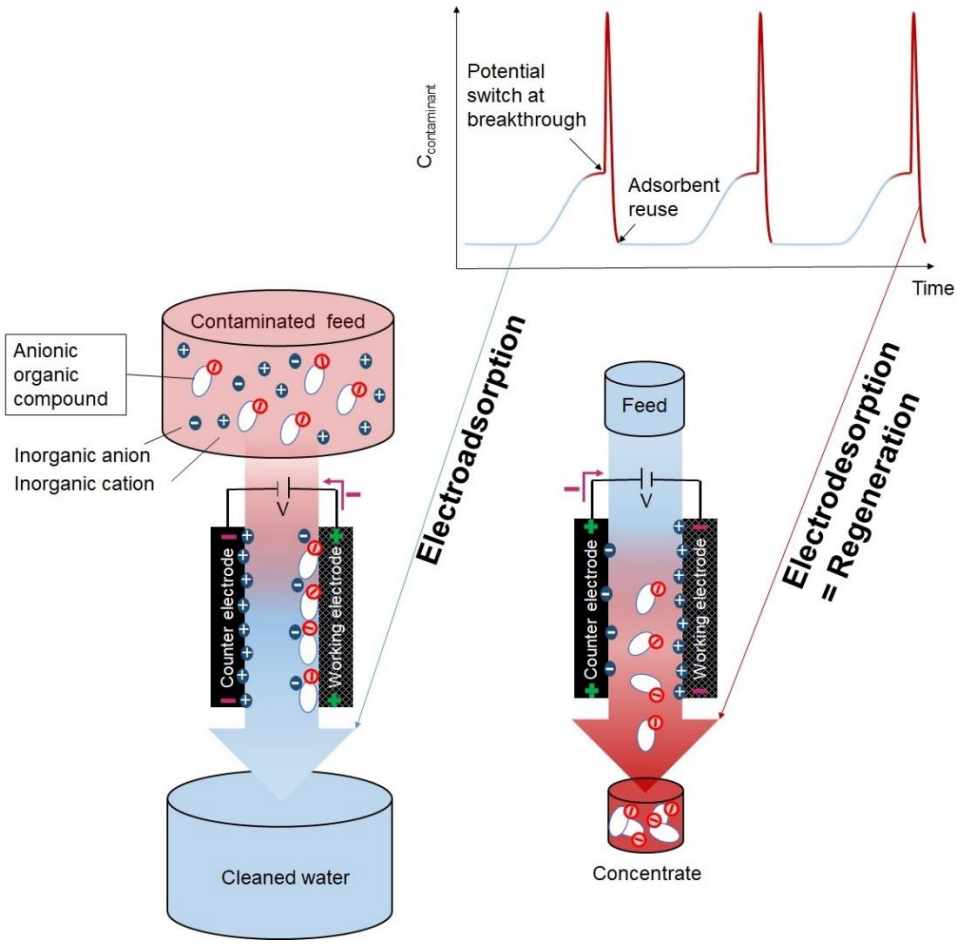

Figure 11. Scheme of water treatment by electroadsorption (left) for removal of an anionic organic compound on a porous working electrode and adsorbent regeneration (right) by electrodesorption, producing a low-volume concentrate.

All studies published on EOC in continuous mode reported i) maximum removal efficiency as pollutant's effluent concentration (C_{out}) divided by inflow concentration (C_{in}) which is achieved in the initial period of the flow-through experiment and ii) adsorbed amount of contaminant (m_{ads}, g) or adsorption capacity (q_{BT}, mg/g) when nearly complete breakthrough (BT) occurred ($C_{out} = C_{in}$) calculated by **Eq. 11** with V_{in} as inflow volume and V_{BT} as complete breakthrough volume:

$$m_{ads} = C_{in} \times V_{in} - \int_{V=0}^{V=V_{BT}} (C_{out})\, dV \qquad (11)$$

Normalizing m_{ads} by the adsorbent electrode mass results in $q_{BT} = m_{ads}/m_{adsorbent}$.

Table 3 lists the removal efficiencies, adsorption capacities, and adsorption coefficients in continuous EOC from some studies. In all examples listed in **Table 3**, the removal efficiency of the ionic OCs was significantly improved by applying a bias potential of the opposite sign to the carbon electrode. This effect can be due to accelerated sorption kinetics and/or enhanced sorption affinity (shift in sorption equilibrium), as both effects can lead to a higher removal degree during the residence time of the liquid in the adsorbent unit.

In addition, all authors reported that adsorbent loading at nearly complete breakthrough increased significantly by potential application. Loading q_{BT} is independent of the amount of adsorbent applied but still varies with compound concentration in the inflow (C_{in}). In contrast, sorption coefficients and retardation factors will be described below as intensive parameters that allow easier comparison among different studies. When nearly complete breakthrough of the adsorbate is achieved in a flow-through adsorbent system, then the adsorbent is equilibrated with the aqueous phase inflow concentration of the adsorbate, and the adsorption coefficient at complete breakthrough ($K_{d,\,BT}$) can be calculated using **Eq. 12**:

$$K_{d,\,BT} = \frac{q_{BT}}{C_{BT}} \tag{12}$$

where C_{BT} (mg/L) is the concentration of the adsorbate in outflow water ($C_{BT} \approx C_{in}$). We applied this calculation for the studies listed in **Table 3** from the information provided in the sources. Before discussing these data, we want to emphasize an alternative approach for evaluating breakthrough curves based on the retardation factor (R factor). This approach allows comparing adsorption performance in cases when, for example, no full breakthrough curve ($C_{out} < C_{in}$) is available. R factor describes the relative transport rates u_w and u (m/s) of water (or a non-retarded tracer) and a sorption-active compound, respectively, through an adsorption unit. R factor can be determined according to **Eq. 13** for an ideal step-function breakthrough curve [124].

Table 3. Removal efficiencies, adsorption capacities, and adsorption coefficients in continuous-mode EOC studies.

Compound / C_{in} (mg/L) / dominant form	**Type of flow cell / flow rate / HRT [d]**	**Volume of treated water at full breakthrough (L)**	**Removal efficiency (%)**	**q_{BT} (mg/g)**	**$K_{d,\,BT}$ [f] (L/kg)**	**$K_{d,\,R}$ [g] (L/kg)**
PFOA / 0.05 / anion [a]	flow-by / not mentioned / 30 min [a]	3.1 (E_{OCP}) 4.2 (+1000 mV, cell voltage) [a]	47 (E_{OCP}) 89 (+1000 mV, cell voltage) [a]	0.067 (E_{OCP}) 0.326 (+1000V, cell voltage) [a]	1,300 (E_{OCP}) 6,500 (+1000V, cell voltage)	some information for calculation missing
PFOS / 0.05 / anion [a]	flow-by / not mentioned / 30 min [a]	3.3 (E_{OCP}) 5 (+1000 mV, cell voltage) [a]	52 (E_{OCP}) 90 (+1000 mV, cell voltage) [a]	0.089 (E_{OCP}) 0.385 (+1000V, cell voltage) [a]	1,800 (E_{OCP}) 7,700 (+1000V, cell voltage)	some information for calculation missing
benzoic acid / 24 / anion [b]	flow-through / 0.6 L / h [b] / not mentioned	1 (E_{OCP}) 1.5 (+800 mV) 0.4 (-700 mV) [b]	52 (E_{OCP}) 74 (+800 mV) 15 (-700 mV) [b]	302 (E_{OCP}) 440 (+800 mV) 100 (-700 mV) [b]	12,600 (E_{OCP}) 18,300 (+800 mV) 6,500 (-700 mV)	some information for calculation missing
sulfadimethoxine / 10 / anion [c]	swiss roll / 1.2 L / h [c] / 27 min [e]	90 (E_{OCP}) 400 (+1000 mV, cell voltage) [c]	99 (E_{OCP}) 99.9 (+1000 mV, cell voltage) [c]	45.5 (E_{OCP}) 203 (+1000 mV, cell voltage) [c]	4,500 (E_{OCP}) 20,300 (+1000 mV, cell voltage)	3,500 (E_{OCP}) 21,000 (+1000 mV, cell voltage)
ciprofloxacin / 10 / cation [c]	swiss roll / 1.2 L / h [c] / 27 min [e]	101 (E_{OCP}) 360 (+1000 mV, cell voltage) [c]	98.9 (E_{OCP}) 99.9 (+1000 mV, cell voltage) [c]	41.5 (E_{OCP}) 192 (-1000 mV, cell voltage) [c]	4,100 (E_{OCP}) 19,200 (-1000 mV, cell voltage)	3,600 (E_{OCP}) 20,000 (-1000 mV, cell voltage)
clarithromycin / 10 / cation [c]	swiss roll / 1.2 L / h [c] / 27 min [e]	56 (E_{OCP}) 165 (+1000 mV, cell voltage) [c]	98.1 (E_{OCP}) 99.9 (+1000 mV, cell voltage) [c]	13 (E_{OCP}) 71 (–1000 mV, cell voltage) [c]	1,300 (E_{OCP}) 7,100 (-1000 mV, cell voltage)	2,100 (E_{OCP}) 8,400 (-1000 mV, cell voltage)

All potentials are vs. SHE, otherwise, it was mentioned. [a] [123], [b] [91], [c] [28]. [d] Hydraulic retention time or residence time as the time that a fluid parcel of water needs to pass the unit. [e] Calculated by us from the information provided in the study. [f] We calculated the $K_{d,\,BT}$ values at complete breakthrough by **Eq. 12**. [g] We calculated $K_{d,\,R}$ values from retardation factor by **Eq. 13**.

$$\text{R factor} = \frac{u_w}{u} = \frac{V_{ads}}{V_{void}} = 1 + \frac{m_{solid}}{V_{void}} \times K_{d,\,R} \quad (13)$$

with V_{ads} as breakthrough water volume and V_{void} as water-filled void volume of the adsorbent unit. R factor also equals the number of exchanged void volumes until breakthrough of the adsorbate occurs. $\frac{m_{solid}}{V_{void}}$ (in kg/L) is the adsorbent mass/water volume ratio in the adsorbent unit, and $K_{d,\,R}$ (in L/kg) is the sorption coefficient of the adsorbate. Note that m_{solid} and $K_{d,\,R}$ need to refer to the same solid, either the whole solid mass (e.g., for a composite electrode) or its sorption-active fraction. When sorption isotherms are non-linear, $K_{d,\,R}$ is an effective value inherent to the relevant inflow concentration of the compound used in the flow experiment: $K_{d,\,R} = C_{in}^{n_{ads}-1} \times K_F$ where K_F and n_{ads} are the Freundlich adsorption coefficient and Freundlich exponent of the adsorbate determined in batch experiments.

For rapid small-scale tests, breakthrough curves are typically not ideal step functions but rather S-shaped due to dispersion effects, slow pore diffusion, or rate-limited sorption/desorption steps. Thus, in a simplified approach, the 50%-breakthrough volume ($V_{50\%\,ads}$) is often used as V_{ads} to calculate R factors according to **Eq. 14**.

If $K_d \times \frac{m_{solid}}{V_{void}} >> 1$ (as typical for exploitable adsorption effects), it holds:

$$\text{R factor} \approx \frac{m_{solid}}{V_{void}} \times K_d \quad (14)$$

Thus, sorption coefficients can also be calculated from retardation factors using **Eqs. 13** or **14** in breakthrough experiments. Here we assign an index R for sorption coefficients $K_{d,\,R}$ determined in this way. Under idealized conditions (nearly step-function breakthrough curve) $K_{d,\,BT}$ and $K_{d,\,R}$ are equal to the sorption coefficient K_d determined under equilibrium conditions for C_{in} of the compound.

Figure 12 shows the enhancement factors in q_{BT} (values provided in **Table 3**) induced by the applied potential in the reviewed continuous mode electrosorption experiments.

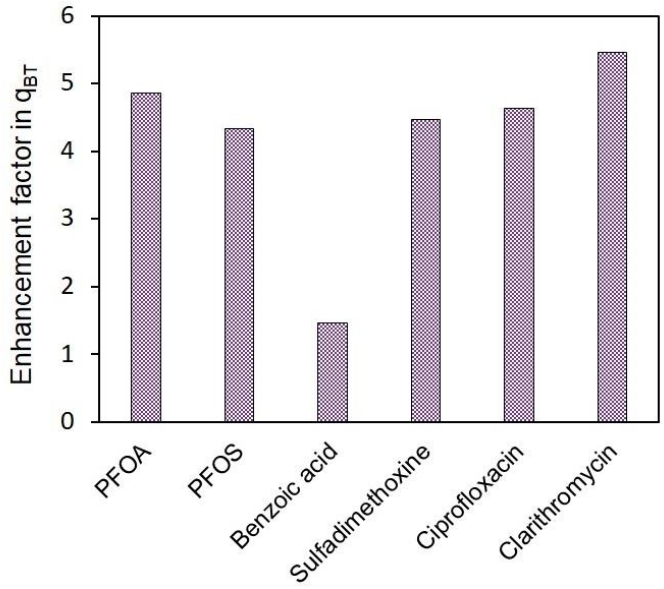

Figure 12. Enhancement factor in q_{BT} for EOC at carbon electrode potential opposite to compound charge compared to E_{OCP} conditions. For experimental conditions and references, see **Table 3**.

For all studied cationic and anionic compounds, a significant improvement in adsorption capacities with a 4-fold to 6-fold increase in q_{BT} was observed when the adsorbent was charged using bias potentials of the opposite sign. An exception was benzoic acid, where the increase related to E_{OCP} conditions was only of a factor of 1.5. As the authors have not reported E_{OCP} and E_{PZC} of the used AC electrode, it is unclear whether a favorable positive net charge of the electrode already at E_{OCP} could be the reason for this limited effect. A stronger modulation of adsorption was obtained in the case of benzoic acid by counter-charging (+800 mV vs. SHE) and co-charging (-700 mV vs. SHE) of the adsorbent electrode (**Table 3**), which resulted in a factor of 4 change in q_{BT}. This is especially important when focusing on electrosorption for on-site adsorbent regeneration.

One of the most important parameters in evaluation of continuous EOC is the concentration or enrichment factor. The enrichment factor addresses the performance of the EOC process in concentrating an OC from a large volume of contaminated water by electro*ad*sorption and subsequent electro*de*sorption into a smaller volume of regeneration water (see **Figure 11**). It

quantifies the volume reduction of contaminated water (**Eq. 15**). Surprisingly, this parameter has not been frequently considered in EOC studies so far.

Two scenarios can be considered for desorption: i) a regeneration solution (e.g., tap water or treated effluent from the adsorption unit) free of the contaminant(s) is used as a regeneration solution for desorption. ii) Alternatively, the inflow water to be treated and still containing the original contaminant is used in the desorption step. In scenario i), depending on the volume of water flushed through in the desorption step, almost complete recovery of the contaminant is achieved in case of fully reversible ad-/desorption equilibria on the adsorbent. In contrast, in scenario ii) the degree of desorption or recovery X_{des} is < 1 and depends on the difference in adsorption affinities under ad- and desorption conditions. Which option is more appropriate for a particular water treatment case does also depend on tolerated/allowed discharge limits for the treated water as remaining loading of micropollutants will lower the maximum removal efficiency in the next adsorption step.

For the use of 'clean' water as desorption solvent (scenario i), we derived in a previous study [124] **Eq. 15** to estimate theoretically achievable concentration factors for a flow-through EOC unit. It is based on the Freundlich isotherm parameters K_F and n at the potential applied for adsorption (with subscript ads) and desorption (with subscript des) of targeted contaminants:

$$\frac{V_{ads}}{V_{des}} = \frac{C_{des}}{C_{in}} = C_{in}^{(n_{ads}/n_{des} - 1)} \times \left(\frac{K_{F,\,ads}}{K_{F,\,des}}\right)^{1/n_{des}} \quad (15)$$

C_{des} is the averaged contaminant concentration in the regeneration solution. If under electro*de*sorption conditions, the adsorption affinity of the contaminant is very low, V_{des} (volume of water for desorption) reaches a minimum value that is close to the void volume of the adsorbent unit that needs to be flushed out ($V_{des} \approx V_{void}$):

$$\frac{V_{ads}}{V_{des}} = \frac{m_{solid}}{V_{void}} \times C_{in}^{n_{ads} - 1} \times K_{F,\,ads} \quad (16)$$

Zhou et al. [124] calculated a theoretically achievable enrichment factor of 45 for trifluoroacetic acid (TFA) as contaminant adsorbed on a typical commercial activated carbon felt.

For scenario ii), i.e. using contaminated inflow water as regeneration medium, in another study [29] we derived respective equations **Eq. 17** and **Eq. 18** that relate ad- and desorption water volume ratios and extents of desorption for continuous EOC. Using the concentration factor as performance parameter, we obtain:

$$\frac{V_{des}}{V_{ads}} = \frac{X_{des}}{C_{in}^{a} \times \left(\frac{K_{F,\,ads}}{K_{F,\,des}}\right)^{\frac{1}{n_{des}}} - 1} \qquad \text{with: } a = \frac{n_{ads}}{n_{des}} - 1 \tag{17}$$

X_{des} can be described as follows:

$$X_{des} = 1 - \frac{K_{F,\,des}}{K_{F,\,ads}} \times C_{in}^{b} \qquad \text{with: } b = n_{des} - n_{ads} \tag{18}$$

A value of 115 was calculated as a theoretically achievable concentration factor (V_{ads}/V_{des}) for EOC of TFA using potentials of +300 mV and –800 mV, for the adsorption and desorption step, respectively, on an ACF electrode. The contaminant recovery X_{des} under these conditions was estimated as 95%. For a switch between open circuit and +100 mV, a concentration factor of 41 and X_{des} = 91% were calculated.

Eqs. 15-18 allow estimating concentration factors achievable under ideal conditions based on batch experiment data on the modulation of adsorption performance under equilibrium conditions by electric potentials. Ideal conditions in this respect refer to, for example, fast adsorption/desorption kinetics and low dispersion effects in the adsorbent unit, the absence of disturbance by other water (matrix) components, and no undesired effects of the counter electrode. The sorbent should not retain substantial amounts of the target contaminants released from the carbon-based sorbent upon switching the charging state in the desorption step. Thus, these enrichment factors should be considered as best-case values based on the

potential-induced effects on sorption equilibria. Nevertheless, they build the basis towards continuous mode EOC development in future.

Enrichment factors can also be derived directly from continuous EOC experiments. They are not strictly intrinsic to the adsorbate-adsorbent system, but also depend on some boundary conditions. In a recent study, an operational concentration factor (termed apparent enrichment factor in [124]) was calculated via **Eq. 19**:

$$\text{Operational enrichment factor} = \frac{V_{50\%\ ads}}{V_{95\%\ des}} \times \text{achieved recovery (Re\%)} / 100 \quad (19)$$

where $V_{50\%\ ads}$ is the volume of the water inflow in the (electro)adsorption step up to a 50% breakthrough of the contaminant, and $V_{95\%\ des}$ is the water needed to achieve 95% of the respective recovery (Re%) in the desorption step. Re% is calculated from the amount of target compound desorbed to the total amount adsorbed (**Eq. 20**).

$$Re\% = (m_{des} / m_{ads}) \times 100 \quad (20)$$

where m_{des} (g) and m_{ads} (g) are total amounts of adsorbate desorbed and adsorbed, respectively. An operational enrichment factor of 7.5 and a recovery of 95% were obtained in this way for TFA on ACF using E_{OCP} in the adsorption and -100 mV in the electrodesorption step in a small-scale flow-through reactor [124]. In this case, an oxidized ACF as CE with a lower thickness than the WE showed negligible TFA adsorption even under anodic polarization of CE. Compared to the theoretically achievable concentration factor of 45, as calculated in the same study for an up-scaled unit based on **Eq. 16**, the value from lab-scale experiments is considerably lower. This was explained by the non-optimal m_{solid}/V_{void} ratio in the miniaturized set up.

When applying **Eq. 19**, we calculated an operational enrichment factor of 8.9 for electroad- and desorption (+1000 mV vs. –1000 mV cell voltage) with 96% recovery of sulfadimethoxine in the study published by Wang et al. [28]. The authors used a high water flow rate in the

desorption step to avoid re-adsorption of contaminants by the CE as adsorbent. WE and CE were of the same material but with different thicknesses (three times thinner for the CE). High flow rates in desorption, however, can be detrimental to the achievable concentration factor if the uptake capacity of the regeneration solution is not fully exploited due to incomplete local equilibration. Appropriate CE materials that show negligible solute uptake under desorption conditions are important for ensuring fast and complete regeneration of EOC units. Technically achievable concentration factors in large-scale EOC units are not yet available because most studies remained at the laboratory scale. For example, in large-scale reverse osmosis units, concentration factors typically range from 5 to 7 [125, 126]. The above-listed considerations and examples of theoretically achievable concentration factors illustrate that EOC has great potential as a pre-concentration step before the final degradation of contaminants and for the design of on-site regenerable adsorbents.

The continuing rapid growth of the EOC community necessitates a standardization of key metrics. **Table 4** provides a number of parameters to describe and evaluate the performance of EOC units in continuous operation, which are consistent with previous literature in the field.

6. State-of-the-art of EOC porous electrodes and future electrodes

Our literature review shows that around 70% of all studies published on EOC have applied various types of AC materials as working electrodes. Thereby, half of this 70% are ACF materials, including AC cloth and AC fiber. Several studies reported various inherent problems encountered with electrodes based on conventional AC, such as powder and granular AC, which are either require binders or are used as packed beds (granular AC). Inherent problems include i) a low electrical conductivity, ii) irregular pore structure, iii) large potential as well as pressure drop (in thick electrodes and packed beds), and iv) high electrical or mass transfer resistance, which are related to the shape/geometry of the composite or packed bed electrodes.

Table 4. The evaluative parameters recommended for EOC performance in continuous mode.

	Parameter	**Parameter measurement or method of calculation**
1	adsorbent (porous electrode) mass / void volume ratio of the unit	from design of the adsorber unit
2	hydraulic retention time (HRT) or residence time of the water in the unit in ad- and desorption steps	from design of the adsorber unit
3	space time in L/(L s) or L/(kg s)	water flow per volume or mass of adsorbent bed
4	maximum removal efficiency achieved in the adsorption step	$(1 - C_{out}/C_{in}) \times 100\%$
5	a parameter quantifying the useful operation time such as number of exchanged void volumes or unit volumes until reaching a certain breakthrough limit	volume of inflow water / total or void volume of the unit. Void volume is the water-filled volume in the unit which also determines the residence time of water in the unit. Total volume includes the solid- and water-filled volumes
6	adsorption coefficients in the flow-through adsorption system such as $K_{d,\,BT}$ or $K_{d,\,R}$ to characterize adsorption performance	from experimental data with continuous EOC and **Eqs. 12–13**
7	theoretically achievable concentration factor	from (batch) EOC data under equilibrium conditions and **Eqs. 15–18**
8	operational concentration factors (V_{ads} / V_{des}) if ad- and desorption steps are conducted for adsorbent regeneration	from experimental data with continuous EOC under certain operation conditions and **Eq. 19**
9	contaminant recovery (Re%) as percentage of desorbed adsorbate if ad- and desorption steps are conducted for adsorbent regeneration	from experimental data with continuous EOC and **Eq. 20**

In addition, problems arise from v) the chemistry of the materials, such as binder degradation, vi) changes in textural and surface chemical properties of the carbon and composite structures upon anodic polarization, and vii) channeling, thereby resulting in lower process efficiency and overall adsorption capacity [30, 127]. Some of these problems can be mitigated by using alternative porous carbon materials. At the same time, the sensitivity for surface oxidation is more or less inherent to all carbon-based porous electrode materials and needs to be considered when selecting operation conditions.

Thanks to i) easy handling, ii) high mechanical integrity, iii) electrical conductivity, iv) regeneration potential, and v) very high specific surface area combined with a large outer surface/volume ratio of the µm-sized fibers, ACF materials have numerous advantages compared to AC grains or granules [128, 129]. ACFs are mostly composed of polymer-derived carbon fibers [29, 124, 130]. The materials are composed of high-purity carbon with a low (typically < 10 mass%) non-carbon content [29, 130].

The presence of oxygen and nitrogen on ACFs can be manipulated by surface functionalization [54, 124]. In terms of physical parameters, commercial ACF samples are commonly available in a layer thickness of about 0.5 to 3 mm, a geometrical density of 0.14-0.24 g/cm^3, and specific electrical resistivity of 0.25–1.35 (Ω × cm) which is noticeably lower as compared to the resistivity of 11.5–25 (Ω × cm) of conventional composite electrodes composed of polymer-bound AC powder [124, 130].

Figure 13 shows physical and textural properties of ACF2 from **Figure 8** and the modified samples, which are oxidized ACF2 (OXACF2) and defunctionalized ACF2 (DeACF2). The ACFs are composed of numerous fibers with diameter ≈ 10 µm (**Figure 13a-e**). As can be seen in **Figure 13f**, ACF2, OXACF2, and DeACF2 are microporous, with slightly wider pores for DeACF2 and narrower pores for OXACF2.

A growing number of studies on promising novel applications of ACF materials have been published in the last few years, involving commercial materials in most cases [129]. These materials are specifically attractive for electrochemical applications because they do not require particular shaping (no binders) and can be used directly as free-standing electrodes [128, 130]. Furthermore, it is known that a proper selection of ACF based on its chemical surface and electrochemical properties can significantly enhance the AC electrode stability [29, 48, 103]. In **Section 4.2.2.**, we discussed the challenges towards an effective and efficient application of ACF materials for EOC and proposed an approach based on E_{PZC}.

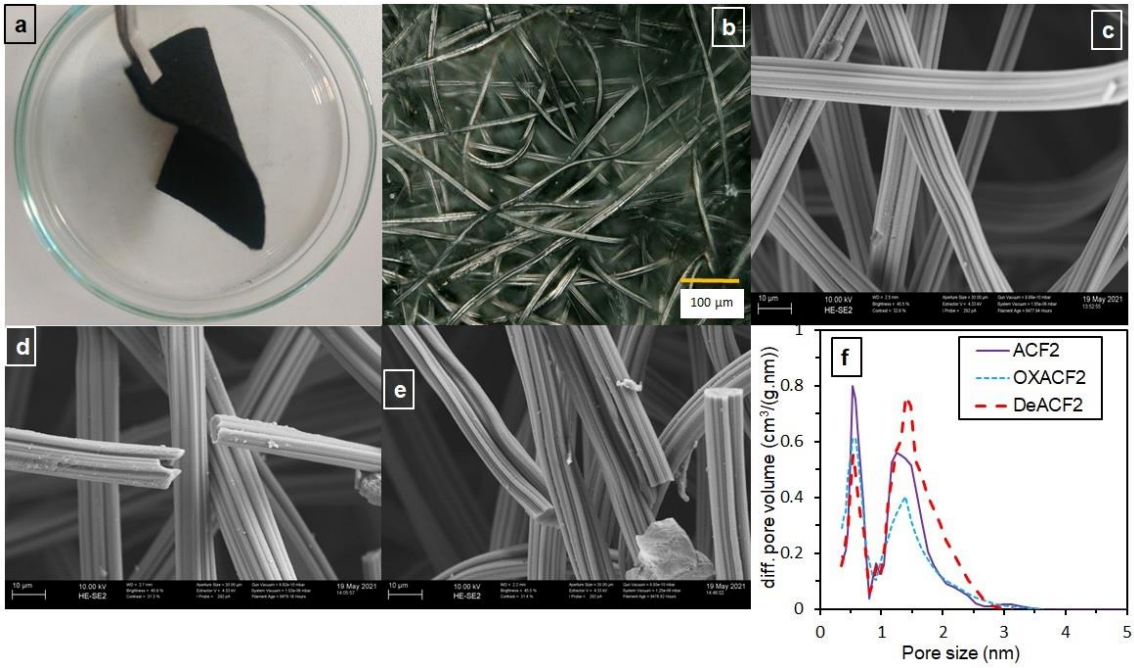

Figure 13. Physical appearance of ACF2 as felt (a) and fibers (b) [131]. Scanning electron microscopy images of ACF2 (c), OXACF2 (d), and DeACF2 (e). Pore size distributions of the ACFs are shown in (f). Reprinted with permission from [17] (c, d, and e) and [124] (d) (copyright 2023, Elsevier).

Beyond ACF, further novel porous electrode materials were applied for EOC, such as CNT [63], CNT/graphene composites [64], Cu/F-rGA [101], and redox copolymers [65]. In general, there is a strong need to develop novel electrode materials for: i) enhancing the adsorption capacity of target OCs, ii) enhancing the adsorption rate of the adsorbates on the porous electrode

upon polarization, iii) enhancing electrode stability over prolonged polarization periods, and iv) enhancing selectivity for targeted OCs.

Recently, PFOA has received increasing interest in EOC studies. Thus, it is a good candidate to compare achievable EOC effects for various adsorbent types which is not possible for other target compounds due to the lack of available studies. **Figure 14a** shows the adsorption coefficients of PFOA on various materials with and without applied potential. PFOA adsorption is influenced more substantially (18-times enhancement in K_d) by applied positive potential on CNT/20%graphene than on other electrode materials, even though on two of the electrodes, Cu/F-rGA and redox copolymers, higher positive potentials were applied. Considering that the parameter E_{eff} could provide a better basis for comparison of the potential effect for the various materials, which is, however, not available from these studies. The highest K_d value for PFOA adsorption was obtained for the positively charged ACF with 10^6 L/kg [29].

Regarding the effect of bias potential on adsorption rate, CNT/20%graphene composite shows the best performance. The data from the literature indicate no significant enhancement in the adsorption rate of PFOA on ACF when a positive potential is applied (+700 mV **Figure 14b**). The adsorption rate of PFOA on two of the novel electrode types (CNT/20%graphene and Cu/F-rGA) was strongly improved by applying +800 mV and +1000 mV, respectively. One reason for the vastly different effect could be the slower diffusion of PFOA due to the narrower pores of ACF (mean pore diameter: 1.5 nm determined by CO_2 adsorption/desorption [29], **Figure 14c**) than in the case of Cu/F-rGA [101] (**Figure 14d**), the CNT [123] (**Figure 14e**), and CNT/20%graphene [64] electrodes with mean pore diameters of 4.5 nm, 3.8 nm to 7.9 nm and 3.1 nm, respectively, all characterized by N_2 adsorption/desorption. Applying microporous ACFs for EOC has an advantage of exerting a size exclusion effect on NOM and thus reduce

competitive adsorption [29]. However, NOM coverage of the external ACF surface can be an issue as well.

As a conclusion, the effects of bias potential on rate constants and K_d are not necessarily correlated. However, there are indications that by using novel mesoporous electrode materials, not only adsorption coefficients but also adsorption rates of ionic OCs can be effectively enhanced by electrosorption.

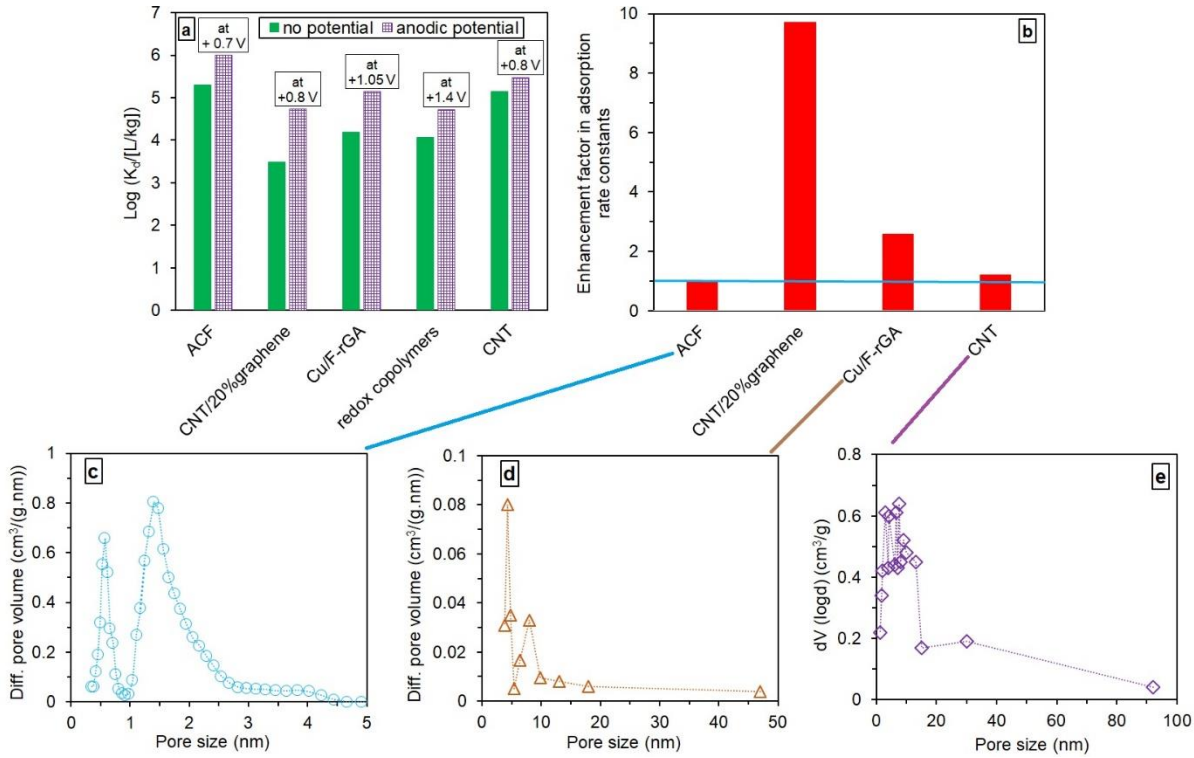

Figure 14. Adsorption coefficient K_d of PFOA on various electrode materials with and without applied potential (a) and impact of potential on adsorption rate constants of PFOA on ACF (k_2), CNT/20%graphene (k_2), Cu/F-rGA (k_1), and CNT (k_2) (b). Pore size distributions of ACF (c) (adopted from [29]), Cu/F-rGA (d) (adopted from [101]), and CNT (e) (adopted from [63]) are shown. All potentials in panel (a) are provided vs. SHE. The kinetics data for redox copolymers were not reported. Pore size distribution for CNT/20%graphene was not reported. For detailed information on the experimental conditions, citations, and calculated parameters, see **Tables 1-2**. Line in (b) represents a factor of 1; that is there is no potential effect.

As already pointed out in **Section 4.2.3.**, future studies on kinetics in EOC should derive rate constants for diffusion in the porous solid as true intrinsic parameters for mechanistic discussions.

The EDL capacity or specific capacitance (C, F/g) of the electrodes is a parameter for evaluating the charge capacity of the electrode in the absence of a Faradaic current. It can be calculated

by various techniques, for example, galvanostatic cycling with potential limitation [130] and cyclic voltammetry (CV) [21]. The studies reviewed here applied CV and **Eq. 21** for calculation of C:

$$C = \frac{S}{2 \times m \times v \times \Delta V} \quad (21)$$

where C is the specific capacitance (F/g), S is the integral area of the CV curve (in W), v is the scan rate (V/s), ΔV is the scan potential range used for integration (V), and m is the mass of the materials loaded (g).

Figure 15 compares q_m in electroadsorption of PFOA on ACF [29], on CNT [63], on CNT/20%graphene [64], and on Cu/F-rGA [101] with the C values of these electrodes. **Figure 15** reveals no straigh correlation between specific capacitance and maximum electroadsorption capacity of an electrode towards an anionic adsorbate such as PFOA.

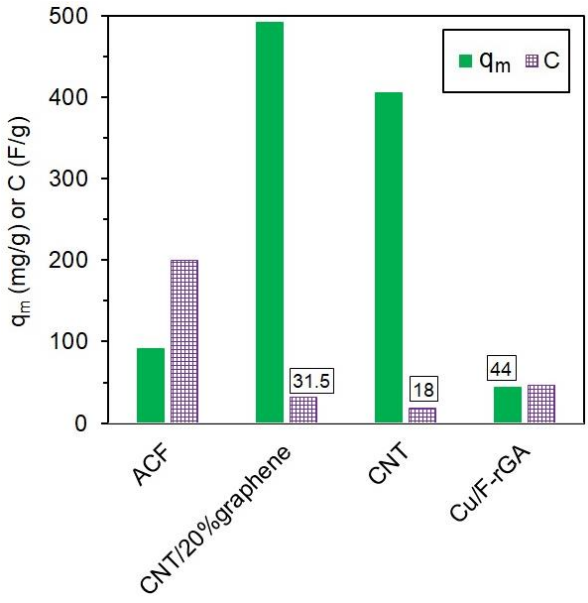

Figure 15. Comparison between maximum electroadsorption capacities (q_m) of PFOA on ACF (at +700 mV) [29], CNT (at +800 mV) [63], CNT/20%graphene (at +800 mV) [64], and Cu/F-rGA (at +1050 mV) [101] with specific capacitance (C) of these electrodes. C values were calculated and reported at potential ranges -300 mV to +700 mV, -1050 mV to +1450 mV, -1250 mV to +1750 mV, and -1250 mV to +1750 mV, respectively. All potentials are provided vs. SHE. For experimental conditions and references, see **Table 1**.

The electrode with the lowest C (CNT/20%graphene) among the electrodes studied here has the highest maximum electroadadsorption capacity of almost 500 mg/g (**Table 1** and **Figure 15**). In terms of adsorption affinity, that is, K_d at low loading, this electrode shows, however, only a moderate performance among all tested materials. As these parameters, that are C, q_m and K_d are all related to specific surface area, cross-correlations are likely. However, as shown here specific capacitance is probably not a key feature for selection of a good electrode for EOC. This is conceivable as, unlike electrosorption of inorganic compounds, electrostatic attraction is only one of several possible driving forces for interactions of carbon-based electrodes with organic ions.

The electric charge (Q, Coulomb) that accumulates in an electrode pair can be converted in moles of electrons using Faraday's number (F number, 96,485 Coulomb/mol) and expressed in as charge density (q_{charge}, mmol/g) (**Eq. 22**) [21]. This value can be compared to the maximum electroadsorption capacity of organic ions (q_m, also expressed in mmol/ g).

$$q_{charge} = \frac{Q}{F\ number} \quad (22)$$

We calculated charge density of the electrodes from data published in some EOC studies [17, 29, 63, 64, 101] and compared it with the respective q_m in EOC. **Figure 16** shows q_m plotted vs. q_{charge}. No correlation is found. C values for ACF electrodes were calculated from CV recorded in narrower potential ranges than those for carbon nanomaterials (potential range in CV ≤ -300 mV to +800 mV against -1050 mV to +1450 mV ≤ potential range in CV ≤ -1250 mV to +1750 mV). For 4 out of 5 (except Cu/F-rGA) EOC experiments using carbon nanomaterial electrodes q_m outperformes q_{charge}. For electroadsorption of PFOA on CNT/20%graphene electrode [64] q_m even exceeds q_{charge}, illustrating again that other mechanisms, such as a strong hydrophobic effect, superimpose electrostatic attractions in adsorption of PFOA and other ionic OCs [26, 54]. For mesoporous adsorbents, adsorption by

hemi-micelle or multilayer formation of long-chain PFAS anions was observed [132], which could also explain the very high maximum loading of almost 50 mass% PFOA on CNT/20%graphene. In such cases, the charge balance between adsorbate and surface is less critical as there is a strong driving force from favorable interactions between the adsorbates, specifically between their hydrophobic fluorinated carbon chains. In contrast, in the case of EOC using ACF electrodes, q_m is always < q_{charge}. In the case of these microporous adsorbents, such multilayer formation is not possible in the internal pore volume, and solute-surface interactions, including charge-balancing and electrostatic interactions, are more important.

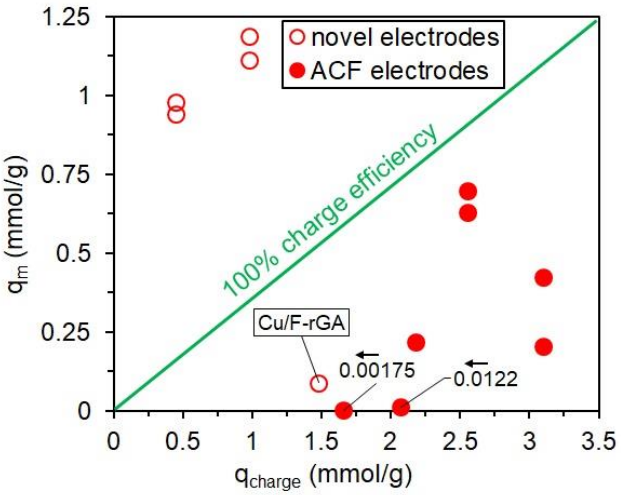

Figure 16. Maximum electroadsorption capacities (q_m) of the selected IOCs vs. the electric charge accumulated (q_{charge}) on the corresponding electrodes. The IOCs are PFOA on ACF (at +700 mV) [29], on CNT (at +800 mV) [63], on CNT/20%graphene (at +800 mV) [64], and on Cu/F-rGA (at +1050 mV) [101], PFBA on ACF (at +700 mV) [29] and on modified ACF (at +450 mV) [29], PFOS on CNT (at +800 mV) [63] and on CNT/20%graphene (at +800 mV) [64], TPA on ACF (+700 mV) [17] and on modified ACF (+600 mV) [17], p-TSO1 on ACF (+700 mV) [17], and p-TSO2 on modified ACF (at +600 mV) [17]. Potentials are provided vs. SHE.

Not all micropores might be accessible for certain organic ions due to their larger size compared to simple inorganic ions. For example, the effective diameter of the molecule relevant for access into cylindrical micropores is 0.6 nm for PFOA [133]. Thus, a lower q_m than q_{charge} can be expected. On the other hand, a highly charged surface can also be detrimental

due to the competition between organic ions and simple inorganic ions (as evident from a bell-shaped K_d vs. potential curve in **Figure 6**).

In contrast to what we observed in **Figure 16** for EOC, in CDI, the salt adsorption always has an increasing trend against q_{charge} [22, 46]. In addition, in CDI the maximum salt adsorption is always < q_{charge} [22, 46], that is, the charge efficiency remains below 100%. We believe that a precise mechanistic study on EOC is plausible while C, q_{charge}, and q_m are measured at the bias potential at which the electroadsorption of the target OC is the highest (**Figure 7**). Thus, a more precise comparison of charge efficiency can also be discussed.

There have been successful laboratory-scale applications of novel porous electrode materials for EOC. However, the industry faces various challenges in producing these nanomaterials: the availability of economically viable technologies, sustainable resource management, and proper market strategies under competitive markets [30, 63]. Nevertheless, the results reviewed here collectively illustrate that EOC performance is strongly material dependent.

In recent years, novel two-dimensional (2D) materials, so-called MXenes, have attracted attention in electrochemical studies such as on CDI [134]. These 2D materials offer benefits such as high surface area, multi-nanolayered structure for fast ion intercalation, functional surface groups for an efficient and fast catch and release of ions, high conductivity, and high pseudocapacitance as well as stability and processing feasibility [134]. In particular, fast catch and release of ions are very attractive features in EOC in principle, ideally represented in the 2D material family. Thus, we suggest considering novel materials, especially 2D materials, in future studies on EOC.

7. A summary on the limitations to EOC and the mitigation strategies

Similar to other electrochemical water purification techniques like CDI, EOC is susceptible to certain limitations that can adversely affect its overall performance. One of the main obstacles

encountered for EOC is the instability in performance over extended durations [17, 29, 124], particularly when AC is used as the electrode material. This instability is primarily attributed to the erosion of electrode materials and properties caused by direct or indirect oxidation and reduction processes occurring even at relatively low potentials (cell voltage < 1.23 V) [128]. As a result, the adsorption performance of the electrodes declines [29] and polarity reversal events, meaning that after extended use the net charge of the electrode is reversed even though the same bias potential is applied due to a shift in its E_{PZC} may occur [48]. Careful selection of suitable ACs based on their E_{PZC} allows the use of the lowest potentials possible for switching between electroadsorption and electrodesorption of PFOA. This selection resulted in a significant improvement in cell stability, increasing the number of adsorption/desorption cycles with stable performance in PFOA removal to 10 [29]. Methods for determining E_{PZC} of AC materials were described in **Section 4.2.2**. In addition, there is a need to develop high surface area adsorption materials with higher stability towards oxidative attack.

The complex nature of emerging organic contaminants (e.g., PMOCs) is a big challenge towards an effective application of EOC for their removal. By means of detailed consideration of compound speciation and surface chemistry of electrode materials, we derived mechanistic insight in the EOC process in **Section 4.2.2**. However, due to the various driving forces and interaction mechanisms potentially involved in OC adsorption, it is currently impossible to estimate the application range of EOC in terms of compound classes. Hence, more research is needed in the best case combined with efforts in modelling. In addition, application of EOC for real water with complex contaminations is a challenge and needs an adjusted treatment strategy. One solution could be based on a multi-step EOC for targeting certain types of OCs in each step. Another strategy could be a specific design of EOC cell for a selective

electrosorption of e.g. anionic OCs and cationic OCs on oppositivelly charged electrodes in a single cell [135]. The combination of EOC with other separation processes is a third option as summarized in the conclusions.

EOC for on-site regeneration and reuse of adsorbents needs to rely on desorption by suitable bias potential. However, in some cases non-electrostatic interactions and other driving forces of OC adsorption can be too strong to be over-compensated by electrostatic repulsion. Such cases can be caused by a strong hydrophobic effect for large non-polar molecules, strong π-π interactions between molecules with condensed aromatic rings and carbon surfaces, and further specific interactions between functional groups of adsorbate and electrode surface or even among adsorbed molecules. Consequently, these interactions can result in incomplete regeneration of the adsorbent or scaling, fouling, and passivation of the electrode surfaces if non-target components are involved. In most cases, however, target compounds with high sorption tendency towards AC are not the critical ones but rather the more hydrophilic, ionic or highly polar compounds, that reduce the effective operation time of AC adsorbers due to early breakthrough. Thus, regular AC adsorbers and EOC units could be beneficially combined. In such a treatment train, AC effectively eliminates first the hydrophobic OCs from the incoming water while the early breakthrough of hydrophilic OCs is prevented by an EOC unit which can be easily regenerated on-site. However, so far there are no studies demonstrating the feasibility of such an approach.

In **Section 4.2.2.**, it was described that the adsorption of PFOA, which is more hydrophobic than PFBA, could be moderately influenced by an external potential. This finding suggests that electrosorption can be applied for certain hydrophobic compounds, as well.

The presence of various components, including dissolved organic matter (DOM), and inorganic ions, introduces adsorption competition in the removal of target organic pollutants by EOC.

The separation of ionic hydrophilic organic compounds, such as (ultra-)short-chain PFAS, becomes particularly challenging in the presence of ions like Cl^-, SO_4^{2-} and NO_3^-. EOC utilizing highly microporous AC electrodes exhibited minimal interference with NOM during the electrosorption of PFOA [29]. This was attributed to a size exclusion effect [29]. Furthermore, a defunctionalized ACF showed selective adsorption of TFA as an ultra-short-chain PFAS with a high adsorption capacity of 30 mg/g in the presence of Cl^-, SO_4^{2-} and NO_3^-. By applying a negative bias potential on the AC electrode, TFA desorption was facilitated in low-ionic-strength aqueous electrolyte solution and showed high recovery rates (≥ 90%) [124]. In the following section, we discuss the limitaions in combining EOC with other techniques.

8. EOC as a combined technique

EOC has been combined with other processes to develop novel technologies for efficient water treatment. Lissaneddine et al. [27] have recently reviewed EOC combinations with photoelectrocatalysis [136], electro-Fenton [137], electrooxidation [65], peroxi-coagulation [138], ultrafiltration [139], electrocatalysis [140], and photocatalysis [141]. We would like to add further the concept(s) of EOC i) driven by microbial electrochemical technologies (MET) [142], ii) combined with other separation processes and, iii) specific combinations of EOC with electrooxidation (ELOX).

<u>EOC and microbial electrochemical technologies:</u> Yang et al. developed an electrosorption unit powered by microbial fuel cells (MFCs) that is the archetype of a MET without electric grid energy consumption. The authors applied this combination for the improved electrosorptive removal of specific contaminants, that are, phenol [92, 143] and tetracycline [144] (both in the mg/L concentration range in inflow water) combined with a reduction in the biodegradable organic load of the wastewater and electricity generation by the MFC.

Electrosorption was also implemented in renewable energy production from wastewater produced in bio-oil production from biomass pyrolysis. EOC was applied to concentrate organic acids such as acetate and propionate from bio-oil washing water and deliver the concentrate to hydrogen production by microbial electrolysis cells (MECs) [38]. These examples illustrate that EOC can be favorably combined with other (microbial) electrochemical processes.

EOC and other separation processes: EOC is a moderately selective process. Strong selectivity can be favorable in specific separation tasks, such as product isolation from the aqueous phase or contaminant removal from water containing non-hazardous organic matrix components. However, in terms of comprehensive water remediation, selectivity can be challenging. For example, applying suitable potentials for organic cations can reduce the adsorption of anions. While such effects can be compensated by using arrays of selective units in sequence, the selectivity issue is more severe in adsorbent regeneration. If not all adsorbed contaminants can be removed in the desorption step, they are transferred into the next adsorption step, where their breakthrough front is moving forward. Thus, EOC alone might only apply to specific contamination problems, such as removing PFAS anions from contaminated groundwater or industrial wastewater with a limited contaminant spectrum. Nevertheless, for more complex contaminations, EOC can be valuable in treatment trains complementing state of the art treatment technologies. For example, EOC units could capture early-breakthrough compounds (hydrophilic ionic compounds) ahead of conventional AC adsorbers and prolong their operation while readily regenerated by a potential switch. Such combinations are, however, still not sufficiently considered.

If inorganic and organic ions are to be simultaneously removed from certain water types, it becomes obvious that there is no strict boundary between CDI and EOC, as both are operated

by similar or the same electrode material and unit design. In a recent study, Lester et al. [145] studied the simultaneous desalination and removal of bisphenol A and estrone (neutral compounds) in a symmetrical undivided electrochemical cell. When applied at a similar concentration, salt adsorption was slightly reduced by the adsorption of the OCs. At the same time, the presence of inorganic ions and the applied potential did not affect the adsorption of the OCs. Afterward, when the electrodes were short-circuited, salt was desorbed into an aqueous brine stream, and subsequently, OCs were desorbed by passing ethanol through the electrodes. When performing CDI and electrosorption of IOCs in a single cell, we need to answer the question: how to avoid the EOC module "just will do CDI"? We suggest two approaches: i) the design of CDI with such small pores that "only" small ions are removed, and ii) going for EOC rather to highly porous materials with outer surface area, such as MXene and graphene. These two approaches can be studied in the future for further developments in combined EOC - CDI processes. For instance, EOC was recently combined with CDI process for simultaneous water deionization and microbial disinfection via electrosorption. This process can be applied in a multi-ion water matrix and is feasible for both pathogenic and biofouling bacteria with up to 90% disinfection efficiency [146, 147].

Zhou et al. [124] studied the removal of TFA (anionic OC) from a tap water matrix containing inorganic anions such as chloride, sulfate, and nitrate in a symmetrical EOC flow cell using a defunctionalized ACF electrode with $pH_{PZC} > 7$ and an oxidized ACF as CE. This study showed that even TFA ,as an extremely hydrophilic organic anion, is much better adsorbed and shows selectively retarded breakthrough compared to the inorganic anions. The uptake of chloride and sulfate was negligible, while nitrate was, to some extent, adsorbed under the applied conditions. In the desorption step, an anodic potential was applied to the defunctionalized ACF, which caused nearly complete desorption of TFA and nitrate so that the electrochemical

cell was regenerated for the next cycle. This work reveals that organic and inorganic anions can be removed simultaneously by electrosorption but the operation time until regeneration can be significantly different. Organic trace contaminants (typically present in sub-µM range) can have much higher retardation factors driven by their high affinity to carbon. In contrast, CDI exploits the non-specific enrichment of inorganic ions (that occur at higher concentrations in the mM range) in the EDL of the charged carbon surface. Thus, regeneration of the carbon's inorganic ion uptake function requires much more frequent potential switches, which would counteract high concentration factors in removing the OCs if only one unit was used. Thus, we believe that two separate units in sequence are a better choice, with an EOC upstream unit (that is 'exhausted' in terms of inorganic ion uptake) and a downstream unit (that is frequently regenerated) for inorganic ion removal (**Figure 17**).

Combination of EOC with ELOX: The combination of EOC and ELOX is appealing because of the synergistic combination of pollutant concentration and destruction or transformation. All studies published on combined EOC-ELOX processes have considered the 'one-reactor' design, that is, using the same system of electrodes for both steps [65, 81, 128].

In this approach, harsh bias potential (>> water electrolysis bias potential) is typically needed for ELOX, which results in the degradation of carbon WEs [29]. Kim et al. [65] proposed electroadsorption / -desorption and then ELOX of PFOA in a single electrochemical reactor by leveraging an asymmetric electrochemical design combining a copolymer-based WE with a boron-doped diamond (BDD) CE. PFOA can be first captured by the WE charged at +1400 mV, whereas, during release (-1000 mV on the WE), the BDD electrode is oxidizing released PFOA at a potential of +4700 mV. Good stability for working under harsh electrochemical conditions was reported for BDD anodes [33, 148]. The stability of the copolymer-based working

electrode (which serves as CE in ELOX step) and cycleability of this process under these conditions are however in question.

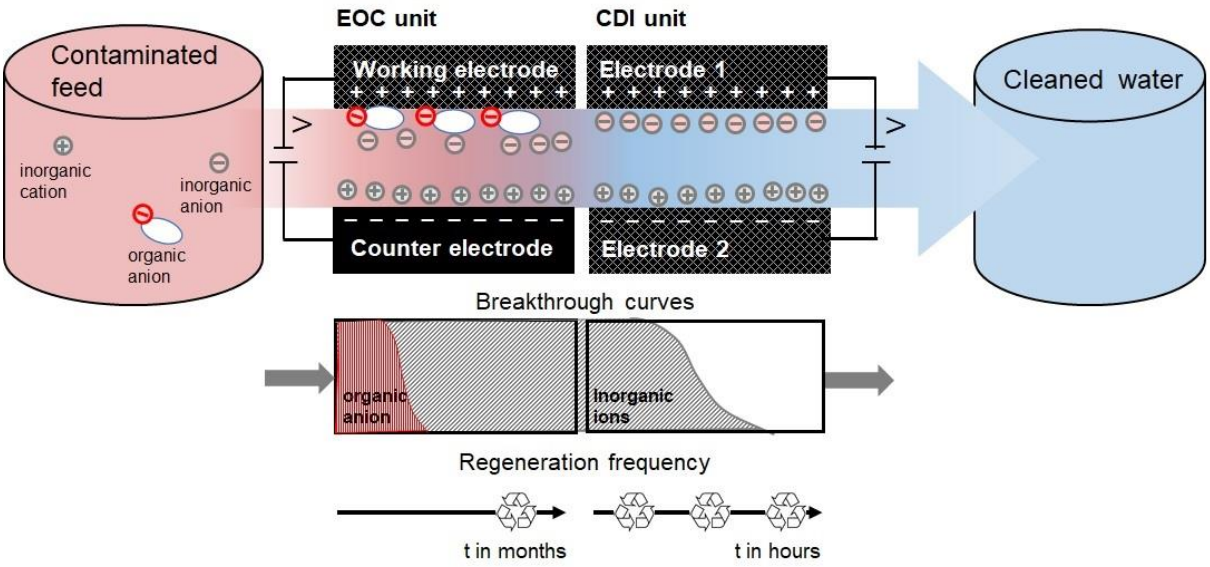

Figure 17. Schematic representation of the combined removal of ionic organic compounds and desalination in a sequence of EOC and CDI units. Ionic organic compounds are more strongly retarded by porous carbon-based adsorbents than inorganic salt water ions. The different regeneration frequencies required argue for using two separate units with more frequent regeneration of the downstream CDI unit.

We believe performing EOC and ELOX in a sequence is an alternative to the ´one-reactor´approach mentioned above. In this case, the first step is the electroadsorptio / -desorption process using mild potentials for adsorption-optimized electrodes. In the second step, electrooxidation is used for treating desorption concentrate in a separate reactor with oxidation-optimized electrodes (e.g., BDD or TiO_x) with higher stability against harsh electrochemical conditions than conventional carbon electrodes. This could be the subject of future research. EOC with post-treatment by ELOX is a synergistic combination, ELOX as valuable destruction technology is challenging for large-volume water treatment and affected by matrix components (e.g., forming undesired byproducts from chloride oxidation). At the same time, EOC can provide selective preconcentration of contaminants into a more suitable water matrix. The combination of the two processes, EOC and ELOX, has a strong potential to

lower the carbon footprint in water treatment technologies. In addition, it can be operated with regenerative electricity and is an alternative to off-site incineration or thermal regeneration as currently applied treatment technologies for spent AC adsorbents [12, 13].

9. Conclusions and future research needs

The field of EOC has experienced enormous growth over the last decade, with ionic organic compounds being essential target compounds. The reason is the urgent need for efficient and sustainable water treatment methods to address the significant problem of ionic and ionizable organic compounds as a large subset of persistent and mobile pollutants in our water cycles. With this review, we assessed potential-induced effects in terms of the desired i) increase in adsorption affinity and capacity, ii) enhancement of adsorption kinetics, and iii) adsorbent regeneration delivering concentrates for post-treatment. This also included whether strong effects are prone to specific compound classes, that is to say, only ionic or ionizable compounds, or apply to a broader compound range, including neutral organic compounds. Beyond that, the continuing rapid growth of EOC research necessitates a standardization of critical metrics. We thus suggest to the EOC community appropriate parameters and terms (**Table 4**) for evaluating the performance of EOC in continuous mode.

Based on the data extracted from the reviewed literature, the impact of bias potential on adsorption *capacity* in most cases is ≤ a factor of 2.5, possibly because q_m is limited by available surface area and pore volume. However, a much more substantial impact of bias potential was observed on sorption coefficients K_d as a measure of adsorption *affinity*. Bias potential can modulate K_d values by a factor of >10 (up to 60) for ionic compounds even in presence of natural organic matter and increased ionic strength, while the impact is always less than a factor of 10 for neutral compounds. Thus, it is evident that EOC can be used to improve the adsorption of in particular charged organic compounds present at low concentrations. The

applicability of EOC for PFAS anions has been recently demonstrated in several studies. At the same time, there is a strong demand for efficient water treatment technologies for this specific compound class as the number of recognized PFAS water contamination sites is steadily increasing worldwide. Together, these two drivers could greatly accelerate the technological development of EOC.

On the other hand, EOC is less likely a *fit-for-all-contaminants* method as other compounds, such as neutral and/or aromatic molecules (adsorbing via multiple non-electrostatic interactions), are less affected by bias potentials. Thus, for treating complex contaminations, such as tertiary treatment of WWTP effluents and water reuse, EOC can be a complementary step in a treatment train where such units can capture early breakthrough compounds ahead of a conventional activated carbon adsorber (lead-lag design). Improving the *ad*sorption performance (affinity and kinetics) is not the only and maybe not even the most essential application of EOC. We see even greater benefit from EOC as a method for regenerating adsorbents on-site, replacing conventional off-site thermal regeneration (or incineration) of conventional AC adsorbents. In this way, EOC may solve the problem of frequent regeneration intervals needed when removing very hydrophilic and, thus, mobile ionic organic compounds from water. In combined lead-lag applications, the bed change intervals of the lag conventional AC adsorbers can be extended, while the lead EOC unit is designed for frequent on-site regeneration. For on-site regeneration of EOC units, strong potential-induced modulation in contaminant adsorption/desoprtion is the key. In this way, EOC is also acting as a pre-concentration technique that can be beneficially combined with subsequent contaminant degradation, for instance, by electrooxidation. EOC even allows to desorb the target contaminants into an electrolyte solution which is beneficial for the subsequent electrooxidation step and avoids adverse effects of water matrix components such as

unwanted oxidation of chloride or bromide. This is an advantage over other pre-concentration techniques such as membrane filtration which at best can concentrate the target contaminant in the original water matrix (nanofiltration) or even concentrates both, inorganic and organic solutes (reverse osmosis). This pre-concentration feature of EOC has not been considered frequently. Nevertheless, we strongly believe that this is an important application field of the technology based on theoretically achievable concentration factors in the range of 40 to 100 predicted from bias potential effects on adsorption equilibria of various perfluorinated alkyl acids (**Section 4.2.2.**), which are considerably higher than the concentration factors (5 to 7) reported for reverse osmosis units. However, putting such high values into practice will require careful design and process engineering to adapt, for example, flow conditions to desorption kinetics and avoid unnecessary dilution of the desorption concentrate. Nevertheless, EOC has the potential to turn carbon-based materials into on-site regenerable adsorbents. Conducting further studies on the utilization of EOC in real wastewater and its selectivity can aid in exploring the feasibility of this method for practical usage concerning diverse water sources.

For EOC to reach tremendous advances, further development in appropriate models and quantitative prediction tools would be highly desirable. The capacitor model of the interface discussed in **Section 3** shows some indications for predicting at least qualitatively the formation of bell-shaped curves when plotting adsorption coefficients (or capacities) against applied bias potentials. Future research may advance prediction tools for EOC based on more recent approaches, such as the mD model (for predominantly microporous electrodes) and the two-dimensional porous electrode theory (for predominantly mesoporous electrodes).

In terms of electrode materials for EOC, more research is needed to understand the role of certain material properties, such as pore structure and chemical surface properties in

enhancing EOC performance. Nevertheless, we were able to show in this review that the potential of zero charge (E_{PZC}) is one of the decisive parameters for a more targeted selection of bias potential in EOC. For example, plots of potential-dependent sorption coefficients from 15 sets of experimental data from literature formed bell-shaped curves with the location of maxima at potentials slightly above the electrode's E_{PZC} for anionic, close to E_{PZC} for neutral, and slightly below E_{PZC} for cationic OCs.

Applying a bias potential can also influence the adsorption kinetics of OCs, with a more substantial impact (up to a factor of 12 increase in rate constants determined by pseudo-first and second-order models) in the case of ionic OCs. Studies on electrosorption of the same compound (PFOA) on various porous electrodes indicate that the adsorption kinetics might be more strongly affected in the case of carbon electrodes with wider pore diameters (mean pore diameter in mesopore range) than for microporous electrodes such as ACF. Faster adsorption kinetics translates into shorter residence times and smaller units for achieving high contaminant removal efficiencies. More comprehensive studies on the individual mass transfer steps in EOC units, including appropriate parameters for film diffusion and internal pore diffusion, are needed. In this respect, effective diffusion coefficients for mass transfer in the porous medium are universal for a specific compound/adsorbent system and less operationally defined than rate constants from empirical pseudo-first- and pseudo-second-order models.

Around 70% of all studies published on EOC have applied various activated carbon materials, with 50% out of 70% activated carbon felts as a porous electrode. Composite electrodes based on carbon nanomaterials (CNTs and graphene-based) and redox-active polymers complement the range of materials studied. Whether these more advanced materials can bring a real breakthrough in EOC application cannot be answered conclusively due to limitations in

comparative studies and uniform evaluation parameters. As EOC results from the superposition of various interaction mechanisms (including electrostatic, non-specific van-der-Waals interactions, and hydrophobicity) common characteristic parameters for electrode performance in CDI (e.g., specific capacitance in F/g and charge capacity in mmol/g) are not simply transferable to EOC. Therefore, future mechanistic studies should consider evaluating the correlation between maximum electroadsorption capacity, C, and q_{charge} at the optimal bias potential for electrosorption (peak maximum in K_d vs. potential curves).

This review illustrates that exploitable potential-induced effects on adsorption are strongly material dependent. Therefore, future research on developing novel materials for high-performance EOC is recommendable. This not only holds for the sorption-active WE but also for suitable CE materials and additional cell components. The role of the CE is often underestimated in EOC studies, even though it strongly affects the potential distribution in the cell and, thus, the cell voltage needed to adjust a particular potential at the WE. Thus, the specific surface area (and/or capacitance) of CE and WE should be of the same magnitude. At the same time, CE materials adsorbing the target compounds can complicate unit regeneration if not two-chamber electrochemical cells are used. Finally, material stability and environmental compatibility are also relevant for CE and all other materials used in EOC cells.

In summary, this review underlines that EOC has the potential to develop a novel water treatment strategy, especially for ionic persistent and mobile contaminants which challenge conventional water treatment technologies. As an electricity-driven pre-concentration process, EOC can further reduce the water treatment footprint as it disconnects carbon-based adsorbents from fossil-fuel-based high-temperature regeneration. This holds especially in combination with destruction technologies that can be easily operated with renewable energy, such as electrooxidation, photocatalysis, sonolysis, and other advanced oxidation

processes with electricity-based production of reactants (e.g., ozone, H_2O_2, persulfates). These benefits encourage future efforts toward technology development for EOC processes combined with techno-economic-ecologic analyses of EOC in future studies.

Acknowledgments

This work was supported by the Helmholtz Association in the frame of the Integration Platform "Tapping nature's potential for sustainable production and a healthy environment" at the UFZ. V.P. thanks Eduard Arzt (INM) for his continuing support.

References

[1] P. Bhatt, G. Bhandari, M. Bilal, Occurrence, toxicity impacts and mitigation of emerging micropollutants in the aquatic environments: Recent tendencies and perspectives, Journal of Environmental Chemical Engineering 10 (2022) 107598.
[2] S.E. Hale, H.P.H. Arp, I. Schliebner, M. Neumann, Persistent, mobile and toxic (PMT) and very persistent and very mobile (vPvM) substances pose an equivalent level of concern to persistent, bioaccumulative and toxic (PBT) and very persistent and very bioaccumulative (vPvB) substances under REACH, Environmental Sciences Europe 32 (2020) 155.
[3] A.T. Besha, A.Y. Gebreyohannes, R.A. Tufa, D.N. Bekele, E. Curcio, L. Giorno, Removal of emerging micropollutants by activated sludge process and membrane bioreactors and the effects of micropollutants on membrane fouling: A review, Journal of Environmental Chemical Engineering 5 (2017) 2395-2414.
[4] J. Margot, L. Rossi, D.A. Barry, C. Holliger, A review of the fate of micropollutants in wastewater treatment plants, WIREs Water 2 (2015) 457-487.
[5] H.P.H. Arp, T.N. Brown, U. Berger, S.E. Hale, Ranking REACH registered neutral, ionizable and ionic organic chemicals based on their aquatic persistency and mobility, Environmental Science: Processes & Impacts 19 (2017) 939-955.
[6] T. Reemtsma, U. Berger, H.P.H. Arp, H. Gallard, T.P. Knepper, M. Neumann, J.B. Quintana, P.d. Voogt, Mind the gap: Persistent and mobile organic compounds—Water contaminants that slip through, Environmental Science & Technology 50 (2016) 10308-10315.
[7] H.P.H. Arp, S.E. Hale, REACH: Improvement of guidance and methods for the identification and assessment of PMT/vPvM substances, Umweltbundesamt, Germany, 2019, pp. 131. https://www.umweltbundesamt.de/publikationen/reach-improvement-of-guidance-methods-for-the.
[8] R. Mailler, J. Gasperi, Y. Coquet, C. Derome, A. Buleté, E. Vulliet, A. Bressy, G. Varrault, G. Chebbo, V. Rocher, Removal of emerging micropollutants from wastewater by activated carbon adsorption: Experimental study of different activated carbons and factors influencing the adsorption of micropollutants in wastewater, Journal of Environmental Chemical Engineering 4 (2016) 1102-1109.
[9] R. Mailler, J. Gasperi, Y. Coquet, S. Deshayes, S. Zedek, C. Cren-Olivé, N. Cartiser, V. Eudes, A. Bressy, E. Caupos, R. Moilleron, G. Chebbo, V. Rocher, Study of a large scale powdered activated carbon pilot: Removals of a wide range of emerging and priority micropollutants from wastewater treatment plant effluents, Water Research 72 (2015) 315-330.
[10] H.N. Phong Vo, H.H. Ngo, W. Guo, T.M. Hong Nguyen, J. Li, H. Liang, L. Deng, Z. Chen, T.A. Hang Nguyen, Poly-and perfluoroalkyl substances in water and wastewater: A comprehensive review from sources to remediation, Journal of Water Process Engineering 36 (2020) 101393. https://doi.org/10.1016/j.jwpe.2020.101393.
[11] D.Q. Zhang, W.L. Zhang, Y.N. Liang, Adsorption of perfluoroalkyl and polyfluoroalkyl substances (PFASs) from aqueous solution - A review, Science of The Total Environment 694 (2019) 133606.
[12] E. Gagliano, M. Sgroi, P.P. Falciglia, F.G.A. Vagliasindi, P. Roccaro, Removal of poly- and perfluoroalkyl substances (PFAS) from water by adsorption: Role of PFAS chain length, effect of organic matter and challenges in adsorbent regeneration, Water Research 171 (2020) 115381.

[13] P. Márquez, A. Benítez, A.F. Chica, M.A. Martín, A. Caballero, Evaluating the thermal regeneration process of massively generated granular activated carbons for their reuse in wastewater treatments plants, Journal of Cleaner Production 366 (2022) 132685.
[14] H. Gu, R. Bergman, N. Anderson, S. Alanya-Rosenbaum, Life-cycle assessment of activated carbon from woody biomass, Wood and Fiber Science (2018).
[15] M.H. Kim, I.T. Jeong, S.B. Park, J.W. Kim, Analysis of environmental impact of activated carbon production from wood waste, Environmental Engineering Research 24 (2019) 117-126.
[16] P. Bayer, E. Heuer, U. Karl, M. Finkel, Economical and ecological comparison of granular activated carbon (GAC) adsorber refill strategies, Water Research 39 (2005) 1719-1728.
[17] J. Zhou, Y. Zhang, M. Balda, V. Presser, F.-D. Kopinke, A. Georgi, Electro-assisted removal of polar and ionic organic compounds from water using activated carbon felts, Chemical Engineering Journal (2021) 133544.
[18] J. Radjenovic, D.L. Sedlak, Challenges and opportunities for electrochemical processes as next-generation technologies for the treatment of contaminated water, Environmental Science & Technology 49 (2015) 11292-11302.
[19] K.Y. Foo, B.H. Hameed, A short review of activated carbon assisted electrosorption process: An overview, current stage and future prospects, Journal of Hazardous Materials 170 (2009) 552-559.
[20] M.A. Ahmed, S. Tewari, Capacitive deionization: Processes, materials and state of the technology, Journal of Electroanalytical Chemistry 813 (2018) 178-192.
[21] M.E. Suss, S. Porada, X. Sun, P.M. Biesheuvel, J. Yoon, V. Presser, Water desalination via capacitive deionization: What is it and what can we expect from it?, Energy & Environmental Science 8 (2015) 2296-2319.
[22] S. Porada, R. Zhao, A. van der Wal, V. Presser, P.M. Biesheuvel, Review on the science and technology of water desalination by capacitive deionization, Progress in Materials Science 58 (2013) 1388-1442.
[23] J.W. Blair, G.W. Murphy, Electrochemical demineralization of water with porous electrodes of large surface area, Saline water conversion, American Chemical Society1960, pp. 206-223.
[24] W. Tang, J. Liang, D. He, J. Gong, L. Tang, Z. Liu, D. Wang, G. Zeng, Various cell architectures of capacitive deionization: Recent advances and future trends, Water Research 150 (2019) 225-251.
[25] J.H. Strohl, K.L. Dunlap, Electrosorption and separation of quinones on a column of graphite particles, Analytical Chemistry 44 (1972) 2166-2170.
[26] M. Kah, G. Sigmund, F. Xiao, T. Hofmann, Sorption of ionizable and ionic organic compounds to biochar, activated carbon and other carbonaceous materials, Water Research 124 (2017) 673-692.
[27] A. Lissaneddine, M.-N. Pons, F. Aziz, N. Ouazzani, L. Mandi, E. Mousset, A critical review on the electrosorption of organic compounds in aqueous effluent – Influencing factors and engineering considerations, Environmental Research 204 (2022) 112128.
[28] S. Wang, X. Li, H. Zhao, X. Quan, S. Chen, H. Yu, Enhanced adsorption of ionizable antibiotics on activated carbon fiber under electrochemical assistance in continuous-flow modes, Water Research 134 (2018) 162-169.
[29] N. Saeidi, F.-D. Kopinke, A. Georgi, Controlling adsorption of perfluoroalkyl acids on activated carbon felt by means of electrical potentials, Chemical Engineering Journal 416 (2021) 129070.
[30] K.Y. Foo, B.H. Hameed, A short review of activated carbon assisted electrosorption process: An overview, current stage and future prospects, Journal of Hazardous Materials 170 (2009) 552-559.
[31] A. Bán, A. Schafer, H. Wendt, Fundamentals of electrosorption on activated carbon for wastewater treatment of industrial effluents, Journal of Applied Electrochemistry 28 (1998) 227-236.
[32] S. Fleischmann, J.B. Mitchell, R. Wang, C. Zhan, D.-e. Jiang, V. Presser, V. Augustyn, Pseudocapacitance: From fundamental understanding to high power energy storage materials, Chemical Reviews 120 (2020) 6738-6782.
[33] J. Radjenovic, N. Duinslaeger, S.S. Avval, B.P. Chaplin, Facing the challenge of poly- and perfluoroalkyl substances in water: Is electrochemical oxidation the answer?, Environmental Science & Technology 54 (2020) 14815-14829.
[34] Y. Han, X. Quan, S. Chen, H. Zhao, C. Cui, Y. Zhao, Electrochemically enhanced adsorption of aniline on activated carbon fibers, Separation and Purification Technology 50 (2006) 365-372.
[35] Y. Han, X. Quan, S. Chen, S. Wang, Y. Zhang, Electrochemical enhancement of adsorption capacity of activated carbon fibers and their surface physicochemical characterizations, Electrochimica Acta 52 (2007) 3075-3081.
[36] Y. Han, X. Quan, X. Ruan, W. Zhang, Integrated electrochemically enhanced adsorption with electrochemical regeneration for removal of acid orange 7 using activated carbon fibers, Separation and Purification Technology 59 (2008) 43-49.
[37] Y. Chen, Y. Tu, Y. Bai, J. Li, J. Lu, Electrosorption enhanced electrooxidation of a model organic pollutant at 3D SnO2-Sb electrode in superimposed pulse current mode, Chemosphere 195 (2018) 63-69.

[38] L.K.-E. Park, S.J. Satinover, S. Yiacoumi, R.T. Mayes, A.P. Borole, C. Tsouris, Electrosorption of organic acids from aqueous bio-oil and conversion into hydrogen via microbial electrolysis cells, Renewable Energy 125 (2018) 21-31.
[39] H. Helmholtz, Ueber einige Gesetze der Vertheilung elektrischer Ströme in körperlichen Leitern mit Anwendung auf die thierisch-elektrischen Versuche, Annalen der Physik 165 (1853) 211-233.
[40] M. Gouy, Sur la constitution de la charge électrique à la surface d'un électrolyte, J. Phys. Theor. Appl. 9 (1910) 457-468.
[41] D.L. Chapman, LI. A contribution to the theory of electrocapillarity, The London, Edinburgh, and Dublin Philosophical Magazine and Journal of Science 25 (1913) 475-481. https://doi.org/10.1080/14786440408634187.
[42] O. Stern, Zur Theorie der elektrolytischen DoppEelschicht, Zeitschrift für Elektrochemie und angewandte physikalische Chemie 30 (1924) 508-516. DOI: 10.1002/BBPC.192400182.
[43] P.M. Biesheuvel, B. van Limpt, A. van der Wal, Dynamic adsorption/desorption process model for capacitive deionization, The Journal of Physical Chemistry C 113 (2009) 5636-5640.
[44] P.M. Biesheuvel, Activated carbon is an electron-conducting amphoteric ion adsorbent, arXiv preprint arXiv:1509.06354 (2015). https://doi.org/10.48550/arXiv.1509.06354.
[45] P.M. Biesheuvel, S. Porada, M. Levi, M.Z. Bazant, Attractive forces in microporous carbon electrodes for capacitive deionization, Journal of Solid State Electrochemistry 18 (2014) 1365-1376.
[46] S. Porada, L. Borchardt, M. Oschatz, M. Bryjak, J.S. Atchison, K.J. Keesman, S. Kaskel, P.M. Biesheuvel, V. Presser, Direct prediction of the desalination performance of porous carbon electrodes for capacitive deionization, Energy & Environmental Science 6 (2013) 3700-3712.
[47] R. Zhao, P.M. Biesheuvel, H. Miedema, H. Bruning, A. van der Wal, Charge efficiency: A functional tool to probe the double-layer structure inside of porous electrodes and application in the modeling of capacitive deionization, The Journal of Physical Chemistry Letters 1 (2010) 205-210.
[48] X. Gao, A. Omosebi, J. Landon, K. Liu, Surface charge enhanced carbon electrodes for stable and efficient capacitive deionization using inverted adsorption–desorption behavior, Energy & Environmental Science 8 (2015) 897-909.
[49] X. Gao, S. Porada, A. Omosebi, K.L. Liu, P.M. Biesheuvel, J. Landon, Complementary surface charge for enhanced capacitive deionization, Water Research 92 (2016) 275-282.
[50] M.A. Montes-Moran, D. Suarez, J.A. Menendez, E. Fuente, On the nature of basic sites on carbon surfaces: An overview, Carbon 42 (2004) 1219-1225.
[51] M.A. Montes-Morán, J.A. Menéndez, E. Fuente, D. Suárez, Contribution of the basal planes to carbon basicity: An ab initio study of the H_3O^+–π Interaction in cluster models, The Journal of Physical Chemistry B 102 (1998) 5595-5601.
[52] I. Cohen, E. Avraham, M. Noked, A. Soffer, D. Aurbach, Enhanced charge efficiency in capacitive deionization achieved by surface-treated electrodes and by means of a third electrode, The Journal of Physical Chemistry C 115 (2011) 19856-19863.
[53] S. Salvestrini, L. Ambrosone, F.-D. Kopinke, Some mistakes and misinterpretations in the analysis of thermodynamic adsorption data, Journal of Molecular Liquids 352 (2022) 118762.
[54] N. Saeidi, F.-D. Kopinke, A. Georgi, What is specific in adsorption of perfluoroalkyl acids on carbon materials?, Chemosphere (2020) 128520.
[55] V.M. Fischer, In situ electrochemical regeneration of activated carbon, PhD dissertation, University of Groningen, Gronengen, Netherlands, 2001. https://research.rug.nl/en/publications/in-situ-electrochemical-regeneration-of-activated-carbon.
[56] A.N. Frumkin, Über die Beeinflussung der Adsorption von Neutralmolekülen durch ein elektrisches Feld, Zeitschrift für Physik 35 (1926) 792-802.
[57] E.M. Gutman, Thermodynamic aspects of capillarity and electrocapillarity of solid interfaces, Journal of Solid State Electrochemistry 20 (2016) 2929-2950.
[58] W.M. Haynes, CRC Handbook of Chemistry and Physics, 95th ed., CRC Press., Boca Raton, 2014. https://doi.org/10.1201/b17118.
[59] Y. Han, X. Quan, S. Chen, H. Zhao, C. Cui, Y. Zhao, Electrochemically enhanced adsorption of phenol on activated carbon fibers in basic aqueous solution, Journal of Colloid and Interface Science 299 (2006) 766-771.
[60] S. Biniak, A. Świątkowski, M. Pakuła, M. Sankowska, K. Kuśmierek, G. Trykowski, Cyclic voltammetric and FTIR studies of powdered carbon electrodes in the electrosorption of 4-chlorophenols from aqueous electrolytes, Carbon 51 (2013) 301-312.
[61] A.S. Pavitt, E.J. Bylaska, P.G. Tratnyek, Oxidation potentials of phenols and anilines: correlation analysis of electrochemical and theoretical values, Environmental Science: Processes & Impacts 19 (2017) 339-349.

[62] E. Bayram, E. Ayranci, Structural effects on electrosorptive behavior of aromatic organic acids from aqueous solutions onto activated carbon cloth electrode of a flow-through electrolytic cell, Journal of Electroanalytical Chemistry 683 (2012) 14-20.
[63] X. Li, S. Chen, X. Quan, Y. Zhang, Enhanced adsorption of PFOA and PFOS on multiwalled carbon nanotubes under electrochemical assistance, Environmental Science & Technology 45 (2011) 8498-8505.
[64] Z. Niu, Y. Wang, H. Lin, F. Jin, Y. Li, J. Niu, Electrochemically enhanced removal of perfluorinated compounds (PFCs) from aqueous solution by CNTs-graphene composite electrode, Chemical Engineering Journal 328 (2017) 228-235.
[65] K. Kim, P. Baldaguez Medina, J. Elbert, E. Kayiwa, R.D. Cusick, Y. Men, X. Su, Molecular tuning of redox-copolymers for selective electrochemical remediation, Advanced Functional Materials 30 (2020) 2004635.
[66] C.O. Ania, F. Béguin, Mechanism of adsorption and electrosorption of bentazone on activated carbon cloth in aqueous solutions, Water Research 41 (2007) 3372-3380.
[67] E. Ayranci, B.E. Conway, Removal of phenol, phenoxide and chlorophenols from waste-waters by adsorption and electrosorption at high-area carbon felt electrodes, Journal of Electroanalytical Chemistry 513 (2001) 100-110.
[68] J. Niu, B.E. Conway, Adsorptive and electrosorptive removal of aniline and bipyridyls from waste-waters, Journal of Electroanalytical Chemistry 536 (2002) 83-92.
[69] J. Niu, B.E. Conway, Adsorption of organics onto an high-area C-cloth electrode from organic solvents and organic solvent/water mixtures, Journal of Electroanalytical Chemistry 546 (2003) 59-72.
[70] E. Bayram, E. Ayranci, Electrochemically enhanced removal of polycyclic aromatic basic dyes from dilute aqueous solutions by activated carbon cloth electrodes, Environmental Science & Technology 44 (2010) 6331-6336.
[71] C. Rong, H. Xien, Electrosorption of thiocyanate anions on active carbon felt electrode in dilute solution, Journal of Colloid and Interface Science 290 (2005) 190-195.
[72] E. Bayram, E. Ayranci, Investigation of changes in properties of activated carbon cloth upon polarization and of electrosorption of the dye basic blue-7, Carbon 48 (2010) 1718-1730.
[73] X.-F. Sun, B.-B. Guo, L. He, P.-F. Xia, S.-G. Wang, Electrically accelerated removal of organic pollutants by a three-dimensional graphene aerogel, AIChE Journal 62 (2016) 2154-2162.
[74] B. Janocha, H. Bauser, C. Oehr, H. Brunner, W. Göpel†, Electrosorption on activated carbon textile, Chemical Engineering & Technology 22 (1999) 750-752.
[75] G. Bharath, E. Alhseinat, N. Ponpandian, M.A. Khan, M.R. Siddiqui, F. Ahmed, E.H. Alsharaeh, Development of adsorption and electrosorption techniques for removal of organic and inorganic pollutants from wastewater using novel magnetite/porous graphene-based nanocomposites, Separation and Purification Technology 188 (2017) 206-218.
[76] F. Yue, Q. Zhang, L. Xu, Y. Zheng, C. Yao, J. Jia, W. Leng, S. Hou, Porous reduced graphene oxide/single-walled carbon nanotube film as freestanding and flexible electrode materials for electrosorption of organic dye, ACS Applied Nano Materials 2 (2019) 6258-6267.
[77] H. Yu, M. Che, B. Zhao, Y. Lu, S. Zhu, X. Wang, W. Qin, M. Huo, Enhanced electrosorption of rhodamine B over porous copper-nickel foam electrodes modified with graphene oxide/polypyrrole, Synthetic Metals 262 (2020) 116332.
[78] D. Wu, Y. Zhao, Q. Liu, C.-C. Chang, W. Hou, Electrosorption of methylene blue from aqueous solution on graphene-titanium electrode: Adsorption kinetics studies, International Journal of Chemical Reactor Engineering 17 (2019) 20180025.
[79] J.M. Serrano, A.U. Khan, T. Liu, Z. Xu, A.R. Esker, G. Liu, Capacitive organic dye removal by block copolymer based porous carbon fibers, Advanced Materials Interfaces 7 (2020) 2000507.
[80] E. Bayram, C. Karaman, Z. Kuru, O. Karaman, Electrosorptive disinfection of Escherichia coli (E. coli) aqueous solutions by activated carbon monolith electrodes, Water Supply (2020).
[81] S. López-Bernabeu, R. Ruiz-Rosas, C. Quijada, F. Montilla, E. Morallón, Enhanced removal of 8-quinolinecarboxylic acid in an activated carbon cloth by electroadsorption in aqueous solution, Chemosphere 144 (2016) 982-988.
[82] E. Bayram, N. Hoda, E. Ayranci, Adsorption/electrosorption of catechol and resorcinol onto high area activated carbon cloth, Journal of Hazardous Materials 168 (2009) 1459-1466.
[83] H.Y. Li X, She D, Shen W-B,, Modified activated carbon fiber felt for the electrosorption of norfloxacin in aqueous solution, Sustainability 12(10) (2020) 3986.
[84] J. Niu, B.E. Conway, Development of techniques for purification of waste waters: Removal of pyridine from aqueous solution by adsorption at high-area C-cloth electrodes using in situ optical spectrometry, Journal of Electroanalytical Chemistry 521 (2002) 16-28.

[85] Y. Han, X. Quan, H. Zhao, S. Chen, Y. Zhao, Kinetics of enhanced adsorption by polarization for organic pollutants on activated carbon fiber, Frontiers of Environmental Science & Engineering in China 1 (2007) 83-88.
[86] J. McGuire, C.F. Dwiggins, P.S. Fedkiw, The electrosorption of phenol onto activated carbon, Journal of Applied Electrochemistry 15 (1985) 53.
[87] E. Bayram, Ç. Kızıl, E. Ayrancı, Flow-through electrosorption process for removal of 2,4-D pesticide from aqueous solutions onto activated carbon cloth fixed-bed electrodes, Water Science and Technology 77 (2017) 848-854.
[88] K.T. Chue, G. Grévillot, D. Tondeur, Electrosorption an activated carbon bed, in: M. Suzuki (Ed.) studies in surface science and catalysis, Elsevier1993, pp. 97-104.
[89] R.S. Eisinger, R.C. Alkire, Separation by electrosorption of organic compounds in a flow-through porous electrode: II . Experimental validation of model, Journal of The Electrochemical Society 130 (1983) 93-101.
[90] R.S. Eisinger, G.E. Keller, Electrosorption: A case study on removal of dilute organics from water, Environmental Progress 9 (1990) 235-244.
[91] E. Bayram, E. Ayranci, Electrosorption based waste water treatment system using activated carbon cloth electrode: Electrosorption of benzoic acid from a flow-through electrolytic cell, Separation and Purification Technology 86 (2012) 113-118.
[92] J. Yang, M. Zhou, Y. Zhao, C. Zhang, Y. Hu, Electrosorption driven by microbial fuel cells to remove phenol without external power supply, Bioresource Technology 150 (2013) 271-277.
[93] I. Langmuir, The adsorption of gases on plane surface of glass, mica and platinum, Journal of the American Chemical Society 40 (1918) 1361-1403.
[94] H.N. Tran, S.-J. You, A. Hosseini-Bandegharaei, H.-P. Chao, Mistakes and inconsistencies regarding adsorption of contaminants from aqueous solutions: A critical review, Water Research 120 (2017) 88-116.
[95] H. Freundlich, Über die Adsorption in Lösungen, Zeitschrift für Physikalische Chemie 57U (1907) 385-470. DOI: 10.1515/zpch-1907-5723.
[96] E.M. Sahin, T. Tongur, E. Ayranci, Removal of azo dyes from aqueous solutions by adsorption and electrosorption as monitored with in-situ UV-visible spectroscopy, Separation Science and Technology 55 (2020) 3287-3298.
[97] J. Niu, B.E. Conway, Molecular structure factors in adsorptive removal of pyridinium cations, 1,4-pyrazine and 1-quinoline at high-area C-cloth electrodes for waste-water remediation, Journal of Electroanalytical Chemistry 529 (2002) 84-96.
[98] O. Kitous, A. Cheikh, H. Lounici, H. Grib, A. Pauss, N. Mameri, Application of the electrosorption technique to remove metribuzin pesticide, Journal of Hazardous Materials 161 (2009) 1035-1039.
[99] N. Saeidi, F.-D. Kopinke, A. Georgi, Understanding the effect of carbon surface chemistry on adsorption of perfluorinated alkyl substances, Chemical Engineering Journal 381 (2020) 122689.
[100] F.E. Woodard, D.E. McMackins, R.E.W. Jansson, Electrosorption of organics on three dimensional carbon fiber electrodes, Journal of Electroanalytical Chemistry and Interfacial Electrochemistry 214 (1986) 303-330.
[101] L. Liu, Y. Liu, N. Che, B. Gao, C. Li, Electrochemical adsorption of perfluorooctanoic acid on a novel reduced graphene oxide aerogel loaded with Cu nanoparticles and fluorine, Journal of Hazardous Materials 416 (2021) 125866.
[102] ChemAxon online platform. https://chemicalize.com, 2022 (Accessed 10 June 2022).
[103] I. Cohen, E. Avraham, Y. Bouhadana, A. Soffer, D. Aurbach, Long term stability of capacitive de-ionization processes for water desalination: The challenge of positive electrodes corrosion, Electrochimica Acta 106 (2013) 91-100.
[104] H. Tobias, A. Soffer, The immersion potential of high surface electrodes, Journal of Electroanalytical Chemistry and Interfacial Electrochemistry 148 (1983) 221-232.
[105] D.C. Grahame, The electrical double layer and the theory of electrocapillarity, Chem Rev 41 (1947) 441-501.
[106] C.H. Hou, C. Liang, S. Yiacoumi, S. Dai, C. Tsouris, Electrosorption capacitance of nanostructured carbon-based materials, J Colloid Interface Sci 302 (2006) 54-61.
[107] L.-H. Shao, J. Biener, D. Kramer, R.N. Viswanath, T.F. Baumann, A.V. Hamza, J. Weissmüller, Electrocapillary maximum and potential of zero charge of carbon aerogel, Physical Chemistry Chemical Physics 12 (2010) 7580-7587.
[108] E. Bayram, E. Ayranci, A systematic study on the changes in properties of an activated carbon cloth upon polarization, Electrochimica Acta 56 (2011) 2184-2189.
[109] J.-P. Simonin, On the comparison of pseudo-first order and pseudo-second order rate laws in the modeling of adsorption kinetics, Chemical Engineering Journal 300 (2016) 254-263.
[110] Y.S. Ho, G. McKay, Pseudo-second order model for sorption processes, Process Biochemistry 34 (1999) 451-465.

[111] C. Yao, T. Chen, A new simplified method for estimating film mass transfer and surface diffusion coefficients from batch adsorption kinetic data, Chemical Engineering Journal 265 (2015) 93-99.
[112] B. Liu, M. Finkel, P. Grathwohl, First order approximation for coupled film and intraparticle pore diffusion to model sorption/desorption batch experiments, Journal of Hazardous Materials 429 (2022) 128314.
[113] Y. Zhang, C. Prehal, H. Jiang, Y. Liu, G. Feng, V. Presser, Ionophobicity of carbon sub-nanometer pores enables efficient desalination at high salinity, Cell Reports Physical Science 3 (2022) 100689.
[114] N. Jäckel, P. Simon, Y. Gogotsi, V. Presser, Increase in capacitance by subnanometer pores in carbon, ACS Energy Letters 1 (2016) 1262-1265.
[115] C.E. Webster, R.S. Drago, M.C. Zerner, Molecular dimensions for adsorptives, Journal of the American Chemical Society 120 (1998) 5509-5516.
[116] J.A. Arnot, M.I. Arnot, D. Mackay, Y. Couillard, D. MacDonald, M. Bonnell, P. Doyle, Molecular size cutoff criteria for screening bioaccumulation potential: Fact or fiction?, Integrated Environmental Assessment and Management 6 (2010) 210-224.
[117] L. Zou, L. Li, H. Song, G. Morris, Using mesoporous carbon electrodes for brackish water desalination, Water Research 42 (2008) 2340-2348.
[118] X. Wen, D. Zhang, L. Shi, T. Yan, H. Wang, J. Zhang, Three-dimensional hierarchical porous carbon with a bimodal pore arrangement for capacitive deionization, Journal of Materials Chemistry 22 (2012) 23835-23844.
[119] Weber, W.J., Morris, J.C., Kinetics of adsorption on carbon from solution. Journal Sanitary Engeering Division Proceedings, 1963, 89 (2), 31-60.
[120] P.J. Mayne, R. Shackleton, Adsorption on packed bed electrodes, Journal of Applied Electrochemistry 15 (1985) 745-754.
[121] E. Bayram, Electrosoption of aromatic organic acids from aqueous solutions onto granular activated carbon electrodes for water purification, Journal of Biology and Chemistry 44 (2016) 273-281.
[122] G. Zhou, W. Li, Z. Wang, X. Wang, S. Li, D. Zhang, Electrosorption for organic pollutants removal and desalination by graphite and activated carbon fiber composite electrodes, International Journal of Environmental Science and Technology 12 (2015) 3735-3744.
[123] S. Wang, X. Li, Y. Zhang, X. Quan, S. Chen, H. Yu, H. Zhao, Electrochemically enhanced adsorption of PFOA and PFOS on multiwalled carbon nanotubes in continuous flow mode, Chinese Science Bulletin 59 (2014) 2890-2897.
[124] J. Zhou, N. Saeidi, L.Y. Wick, Y. Xie, F.-D. Kopinke, A. Georgi, Efficient removal of trifluoroacetic acid from water using surface-modified activated carbon and electro-assisted desorption, Journal of Hazardous Materials 436 (2022) 129051.
[125] O. Alrehaili, F. Perreault, S. Sinha, P. Westerhoff, Increasing net water recovery of reverse osmosis with membrane distillation using natural thermal differentials between brine and co-located water sources: Impacts at large reclamation facilities, Water Research 184 (2020) 116134.
[126] A. Subramani, J.G. Jacangelo, Treatment technologies for reverse osmosis concentrate volume minimization: A review, Separation and Purification Technology 122 (2014) 472-489.
[127] T.-Y. Ying, K.-L. Yang, S. Yiacoumi, C. Tsouris, Electrosorption of Ions from Aqueous Solutions by Nanostructured Carbon Aerogel, Journal of Colloid and Interface Science 250 (2002) 18-27.
[128] M. Gineys, R. Benoit, N. Cohaut, F. Béguin, S. Delpeux-Ouldriane, Behavior of activated carbon cloths used as electrode in electrochemical processes, Chemical Engineering Journal 310 (2017) 1-12.
[129] A.L. Cukierman, Development and environmental applications of activated carbon cloths, ISRN Chemical Engineering 2013 (2013) 261523.
[130] C. Kim, P. Srimuk, J. Lee, S. Fleischmann, M. Aslan, V. Presser, Influence of pore structure and cell voltage of activated carbon cloth as a versatile electrode material for capacitive deionization, Carbon 122 (2017) 329-335.
[131] N. Saeidi, Improving adsorption of perfluoroalkyl acids by tailoring surface chemistry of activated carbon and electric potentials, PhD dissertation, Helmholtz Centre for Enviromental Research-UFZ, Department of Environmental Engineering, Leipzig, Germany, 2021. https://www.ufz.de/index.php?en=20939&ufzPublicationIdentifier=25102.
[132] Q. Yu, R. Zhang, S. Deng, J. Huang, G. Yu, Sorption of perfluorooctane sulfonate and perfluorooctanoate on activated carbons and resin: Kinetic and isotherm study, Water Research 43 (2009) 1150-1158.
[133] Y. Inoue, N. Hashizume, N. Yakata, H. Murakami, Y. Suzuki, E. Kikushima, M. Otsuka, Unique physicochemical properties of perfluorinated compounds and their bioconcentration in common carp cyprinus carpio L, Archives of Environmental Contamination and Toxicology 62 (2012) 672-680.
[134] P. Srimuk, F. Kaasik, B. Krüner, A. Tolosa, S. Fleischmann, N. Jäckel, M.C. Tekeli, M. Aslan, M.E. Suss, V. Presser, MXene as a novel intercalation-type pseudocapacitive cathode and anode for capacitive deionization, Journal of Materials Chemistry A 4 (2016) 18265-18271.

[135] F. He, A. Hemmatifar, M.Z. Bazant, T.A. Hatton, Selective adsorption of organic anions in a flow cell with asymmetric redox active electrodes, Water Research 182 (2020) 115963.
[136] Z. Fan, H. Shi, H. Zhao, J. Cai, G. Zhao, Application of carbon aerogel electrosorption for enhanced Bi2WO6 photoelectrocatalysis and elimination of trace nonylphenol, Carbon 126 (2018) 279-288.
[137] Y. Chai, P. Qin, Z. Wu, M. Bai, W. Li, J. Pan, R. Cao, A. Chen, D. Jin, C. Peng, A coupled system of flow-through electro-Fenton and electrosorption processes for the efficient treatment of high-salinity organic wastewater, Separation and Purification Technology 267 (2021) 118683.
[138] W. Yang, M. Zhou, L. Ma, A continuous flow-through system with integration of electrosorption and peroxi-coagulation for efficient removal of organics, Chemosphere 274 (2021) 129983.
[139] T. Mantel, E. Jacki, M. Ernst, Electrosorptive removal of organic water constituents by positively charged electrically conductive UF membranes, Water Research 201 (2021) 117318.
[140] F. Xu, L. Chang, X. Duan, W. Bai, X. Sui, X. Zhao, A novel layer-by-layer CNT/PbO_2 anode for high-efficiency removal of PCP-Na through combining adsorption/electrosorption and electrocatalysis, Electrochimica Acta 300 (2019) 53-66.
[141] B. Ayoubi-Feiz, S. Aber, A. Khataee, E. Alipour, Electrosorption and photocatalytic one-stage combined process using a new type of nanosized TiO_2/activated charcoal plate electrode, Environmental Science and Pollution Research 21 (2014) 8555-8564.
[142] U. Schröder, F. Harnisch, L.T. Angenent, Microbial electrochemistry and technology: Terminology and classification, Energy & Environmental Science 8 (2015) 513-519.
[143] J. Yang, Y. Zhao, C. Zhang, Y. Hu, M. Zhou, Electrosorption driven by microbial fuel cells without electric grid energy consumption for simultaneous phenol removal and wastewater treatment, Electrochemistry Communications 34 (2013) 121-124.
[144] W. Yang, H. Han, M. Zhou, J. Yang, Simultaneous electricity generation and tetracycline removal in continuous flow electrosorption driven by microbial fuel cells, RSC Advances 5 (2015) 49513-49520.
[145] Y. Lester, E. Shaulsky, R. Epsztein, I. Zucker, Capacitive deionization for simultaneous removal of salt and uncharged organic contaminants from water, Separation and Purification Technology 237 (2020) 116388.
[146] K. Laxman, P. Sathe, M. Al Abri, S. Dobretsov, J. Dutta, Disinfection of bacteria in water by capacitive deionization, Frontiers in Chemistry 8 (2020).
[147] W.T. Chang, P.A. Chen, C.Y. Peng, S.H. Liu, H.P. Wang, Capacitive deionization and disinfection of saltwater using nanostructured (Cu–Ag)@C/rGO composite electrodes, Environmental Science: Water Research & Technology 9 (2023) 883-889.
[148] Q. Zhuo, S. Deng, B. Yang, J. Huang, B. Wang, T. Zhang, G. Yu, Degradation of perfluorinated compounds on a boron-doped diamond electrode, Electrochimica Acta 77 (2012) 17-22.